

**Electronic Supplementary Information**

**High Solid-State Fluorescence in Ring-Shaped AEE-Active Tetraphenylsilole Derivatives**

Yuanjing Cai,<sup>\* a,b</sup> Kerim Samedov,<sup>b</sup> Haley Albright,<sup>b</sup> Brian S. Dolinar,<sup>b</sup> Ilia. A. Guzei,<sup>b</sup> Rongrong Hu,<sup>c</sup> Chaocan Zhang,<sup>a</sup> Ben Zhong Tang<sup>c</sup> and Robert West <sup>\*b</sup>

<sup>a</sup>School of Materials Science and Engineering, Wuhan University of Technology, Wuhan 430070, People's Republic of China

<sup>\*</sup>Email for Y.J. Cai.: [gardencyj3@gmail.com](mailto:gardencyj3@gmail.com)

<sup>b</sup>Department of Chemistry, University of Wisconsin-Madison, 1101 University Ave., Madison Wisconsin 53706, United States.

<sup>\*</sup>Email for Prof. R.West.: [west@chem.wisc.edu](mailto:west@chem.wisc.edu)

<sup>c</sup>Department of Chemistry, The Hong Kong University of Science & Technology, Clear Water Bay, Kowloon, Hong Kong, People's Republic of China

**Table of Contents**

1. General experimental details	
2. NMR spectra of Compounds <b>1-3</b>	Figures S1-S9
3. Single Crystal X-ray Crystallography of Compounds <b>1-3</b>	Table S1-S2, Figures S10-S14
4. Infrared Spectra of Compounds <b>1-3</b>	Figures S15-S17
5. UV-Vis and Fluorescence Spectra of Compounds <b>1-3</b> in THF Solution and as crystals	Figures S18-S20
6. Aggregation Enhanced Emission (AEE) of Compounds <b>2-3</b>	Figures S21-S22
7. Relative Fluorescence Quantum Yields of Compounds <b>1-3</b> in THF Solution	Figures S23-S25
8. Absolute Solid State Fluorescence Quantum Yield of Compounds <b>1-3</b>	
9. Interactions of <b>1-3</b> in the unit cell	Figures S26-S30
10. Excited State UV-Vis Calculations and Molecular Orbitals of <b>1-3</b>	Table S3, Figures S31-S33
11. Optimized Geometry of Compounds <b>1-3</b> (single molecule)	Tables S4-S6
12. References	

## General Experimental details

### Measurments

The  $^1\text{H}$  and  $^{13}\text{C}$  NMR spectra were measured on a Bruker Avance III 500 or a Bruker Avance III 400 spectrometer using  $\text{CDCl}_3$  as solvent and tetramethylsilane (TMS:  $\delta=0$  ppm) as internal standard. The  $^{29}\text{Si}$  NMR spectra were recorded on the Bruker Avance III 500 spectrometer using  $\text{CDCl}_3$  as solvent and TMS as internal standard. Exact mass measurement electrospray ionization-time of flight (EMM-ESI-TOF) mass spectra of compounds **1-3** were recorded on a Waters (Micromass) LCT<sup>®</sup> mass spectrometer using  $\text{CH}_3\text{CN}$  as solvent with 3-10mM  $\text{NH}_4\text{OAC}$ . The melting points of **1-3** were measured on a Thomas Hoover Capillary Melting Point Apparatus. Elemental analysis (C and H) was determined by CE-440 Elemental Analyzer. FT-IR spectra were recorded on a Bruker Tensor27 spectrophotometer using PIKE ATR (Attenuated Total Reflectance).

Suitable single crystals of compounds **1-3** were selected under oil under ambient conditions and attached to the tip of a MiTeGenMicroMount<sup>®</sup>. Single crystal X-ray diffraction intensity data were collected in a stream of cold nitrogen at 100K on a Bruker Quazar SMART APEXII diffractometer with Mo  $\text{K}_{\alpha}$  ( $\lambda = 0.71073 \text{ \AA}$ ) radiation, or a Bruker SMART APEXII diffractometer with Cu  $\text{K}_{\alpha}$  ( $\lambda = 1.54178 \text{ \AA}$ ) radiation. The intensity data was integrated using SAINT and corrected for absorption using SADABS routines.<sup>[1]</sup> The structures were solved using direct methods or charge flipping and refined using SHELXL2013 program.<sup>[2]</sup> The details concerning x-ray crystallographic structure solutions and refinement for compounds **1-3** are tabulated in Table S1.

UV-Vis absorption spectra were measured on an Agilent 8453 UV-Visible Spectrophotometer under room temperature. Fluorescence spectra were measured on a Horiba Jobin Yvon Fluorolog<sup>®</sup>-3 spectrofluorometer at room temperature. The relative fluorescence quantum yields of **1-3** in THF solution were determined using quinine sulfate as a standard reference in 0.1N  $\text{H}_2\text{SO}_4$  aqueous solution. The absolute solid state fluorescence quantum yields were determined on a calibrated integrating sphere according to the method described by de Mello et al.,<sup>[3]</sup> using a 325nm CW light from a He-Cd laser for optical pumping, an Ocean Optics USB2000 miniature fiber optics spectrometer and the same procedure reported elsewhere.<sup>[4]</sup>

All calculations reported herein were performed using Gaussian 09 package.<sup>[5]</sup> Density functional (DFT) was employed with 6-31G (d) basis set of B3LYP theory for full geometry optimization of single molecule. Dispersion force-corrected TD-DFT<sup>[6]</sup>/B3LYP/6-31G (d) and the B3LYP/6-31G (d) were used to perform excited state UV-Vis calculation and MO calculations, respectively.

### Chemicals and Synthesis Procedures

The synthesis of 1,1-dichloro-2,3,4,5-tetraphenylsilole was carried out according to a literature procedure<sup>[7]</sup> and purified by crystallization in  $\text{Et}_2\text{O}$ . The hydrolysis of 1,1-dichloro-2,3,4,5-tetraphenylsilole gives yellow powder of 1,1-dihydroxyl-2,3,4,5-tetraphenylsilole according to a literature procedure<sup>[8]</sup>. Triethylamine was purchased from Sigma Aldrich and used as received without further purification. Dichlorodiphenylsilane, dichlorodimethylsilane were purchased from Gelest, Inc and used directly.

**1-(1,4-(1,2,3,4-Tetraphenyl-1,3-butadiene))-3,3,5,5-tetraphenyl Cyclotrisiloxane (1):** A solution of 0.357 ml (1.70 mmol) dichlorodiphenylsilane was added at -20 °C into a 50-ml round-bottom flask containing 0.71g (1.70 mmol) 1,1-dihydroxyl-2,3,4,5-tetraphenylsilole, 0.01 ml (0.56 mmol) water, 0.47 ml (3.40 mmol) triethylamine and 12 ml THF. The reaction was started at -20 °C using ice-NaCl bath, then was allowed to warm up to room temperature and stir for 3 hours. The reaction mixture was filtered and washed with 100 ml THF. After removing the solvent under reduced pressure, 30 ml  $\text{Et}_2\text{O}$  were added and pale yellow crystals of compound **1** were formed under solvent evaporation. Yield: 0.14 g, 11% (based on 1,1-dihydroxyl-2,3,4,5-tetraphenylsilole). M.p. 247.2 °C. Elemental analysis calcd (%) for  $\text{C}_{52}\text{H}_{40}\text{O}_3\text{Si}_3$ : C 78.35, H 5.06; found: C 78.25, H 5.08. UV (THF,  $1.31 \times 10^{-5} \text{ mol/L}$ , r.t.),  $\lambda_{\max}$  (nm) /  $\varepsilon_{\max}$  ( $\text{mol}^{-1}\text{Lcm}^{-1}$ ): 375/0.79  $\times 10^4$ . IR ( $\nu_{\max}/\text{cm}^{-1}$ ): 3070w (C-H<sub>Ar</sub>), 3051w (C-H<sub>Ar</sub>), 3024w (C-H<sub>Ar</sub>), 3001w, 1591m(C=C<sub>Ar</sub>), 1487m, 1440m, 1429m, 1307w, 1130s(Si-C<sub>Ar</sub>), 1118s(Si-C<sub>Ph</sub>), 1085w, 1058w, 1033vs(Si-O-Si), 1014vs(Si-O-Si), 993vs, 964m, 937m, 912m.  $^1\text{H}$  NMR (500.023 MHz,  $\text{CDCl}_3$ ),  $\delta_H$  (TMS, ppm): 7.41-7.36 (m, 12H, Ar-H), 7.22-7.19 (m, 8H, Ar-H), 7.05-6.98 (m, 8H, Ar-H), 6.84-6.79 (m, 12H, Ar-H).  $^{13}\text{C}$  NMR (125.743 MHz,  $\text{CDCl}_3$ ),  $\delta_C$  (TMS, ppm): 154.51, 137.68, 137.45, 134.58, 133.10, 132.09, 130.50, 129.72, 129.26, 128.03, 127.71, 127.50, 126.72, 126.02.  $^{29}\text{Si}$  NMR (99.3796 MHz,  $\text{CDCl}_3$ ),  $\delta_{\text{Si}}$  (TMS, ppm): -28.98, -33.23. EMM-ESI-TOF-MS: m/z calcd. for  $[\text{C}_{52}\text{H}_{40}\text{O}_3\text{Si}_3+\text{H}]^+$ : 797.2359; found 797.2335.

**2,2,6,6-Tetramethyl-4,4,8,8-bis(1,4-(1,2,3,4-tetraphenyl-1,3-butadiene)) Cyclotetrasiloxane (2)** A solution of 0.565 ml (4.69 mmol) dichlorodimethylsilane was added at -20 °C into a 100-ml round-bottom flask containing 3.92g (9.38 mmol) 1,1-dihydroxyl-2,3,4,5-tetraphenylsilole, 1.31 ml (9.38 mmol) triethylamine and 40 ml THF. The reaction was started at -20 °C using ice-NaCl bath, then was allowed to warm up to room temperature and stir for 3 hours. The reaction mixture was filtered and washed with 120 ml THF. After removing the solvent under reduced pressure, 40 ml  $\text{Et}_2\text{O}$  were added and pale yellow crystals of compound **2** were formed under solvent evaporation. A solvatomorph (**S1**) of compound **2** was also found. Yield: 0.20 g, 9% (based on 1,1-dihydroxyl-2,3,4,5-tetraphenylsilole and dichlorodimethylsilane). M.p. >300 °C. Elemental analysis calcd (%) for  $\text{C}_{60}\text{H}_{52}\text{O}_4\text{Si}_4$ : C 75.91, H 5.52; found: C 75.25, H 5.49. UV (THF,  $1.07 \times 10^{-5} \text{ mol/L}$ , r.t.),  $\lambda_{\max}$  (nm) /  $\varepsilon_{\max}$  ( $\text{mol}^{-1}\text{Lcm}^{-1}$ ): 366/1.27

$\times 10^4$ . IR ( $\nu_{\text{max}}$ /cm $^{-1}$ ): 3070w (C-H $_{Ar}$ ), 3057w (C-H $_{Ar}$ ), 3020w (C-H $_{Ar}$ ), 2966w (C-H $_{Me}$ ), 1595m (C=C $_{Ar}$ ), 1573m (C=C $_{Ar}$ ), 1487m, 1440m, 1303m, 1257s (Si-C $_{Me}$ ), 1232s, 1205s, 1180s, 1151s, 1087vs (Si-O-Si), 1070vs (Si-O-Si), 1062vs, 983s, 910w, 837s, 804s, 788s, 761s.  $^1\text{H}$  NMR (400.182 MHz, CDCl $_3$ ),  $\delta_H$  (TMS, ppm): 7.18-7.12 (m, 12H, Ar- $H$ ), 7.04-6.98 (m, 20H, Ar- $H$ ), 6.82-6.80 (m, 8H, Ar- $H$ ), -0.32 (s, 12H, Si-CH $_3$ ).  $^{13}\text{C}$  NMR (100.635 MHz, CDCl $_3$ ),  $\delta_C$  (TMS, ppm): 153.45, 138.63, 137.99, 133.19, 129.83, 128.98, 127.93, 127.42, 126.45, 125.85, 0.  $^{29}\text{Si}$  NMR (99.3796 MHz, CDCl $_3$ ),  $\delta_{Si}$  (TMS, ppm): -15.50, -42.01. EMM-ESI-TOF-MS: m/z calcd. for [C $_{60}$ H $_{52}$ O $_4$ Si $_4$ +H] $^+$ : 949.3016; found 949.2991.

**2,2,6,6-Tetraphenyl-4,4,8,8-bis(1,4-(1,2,3,4-tetraphenyl-1,3-butadiene)) Cyclotetrasiloxane (3)** A solution of 0.41 ml (1.94 mmol) dichlorodiphenylsilane was added at -20 °C into a 50-ml round-bottom flask containing 1.62g (3.88 mmol) 1,1-dihydroxyl-2,3,4,5-tetraphenylsilole, 0.54 ml (3.88 mmol) triethylamine and 24 ml THF. The reaction was started at -20 °C using ice-NaCl bath, then was allowed to warm up to room temperature and stir for 3 hours. The reaction mixture was filtered and washed with 100 ml THF. After removing the solvent under reduced pressure, 40 ml Et $_2$ O were added and pale yellow crystals of compound 3 were formed under solvent evaporation. Yield: 0.24 g, 21% (based on 1,1-dihydroxyl-2,3,4,5-tetraphenylsilole and dichlorodiphenylsilane). M.p. >300 °C. Elemental analysis calcd (%) for C $_{80}$ H $_{60}$ O $_4$ Si $_4$ : C 80.23, H 5.05; found: C 79.83, H 5.01. UV (THF, 8.12  $\times 10^{-6}$  mol/L, r.t.),  $\lambda_{\text{max}}$  (nm) /  $\epsilon_{\text{max}}$ (mol $^{-1}$ Lcm $^{-1}$ ): 370/1.52  $\times 10^4$ . IR ( $\nu_{\text{max}}$ /cm $^{-1}$ ): 3074w (C-H $_{Ar}$ ), 3049w (C-H $_{Ar}$ ), 3020w (C-H $_{Ar}$ ), 1591m (C=C $_{Ar}$ ), 1571m (C=C $_{Ar}$ ), 1485m, 1440m, 1429m, 1313m, 1303m, 1116vs (Si-C $_{Ph}$ ), 1097vs (Si-O-Si), 1062s (Si-O-Si), 1033s, 1026s, 995s, 943m, 914m, 841w, 790m, 763m, 740m.  $^1\text{H}$  NMR (400.182 MHz, CDCl $_3$ ),  $\delta_H$  (TMS, ppm): 7.31-7.21 (m, 12H, Ar- $H$ ), 7.07-6.95 (m, 24H, Ar- $H$ ), 6.80-6.73 (m, 16H, Ar- $H$ ), 6.60-6.58 (m, 8H, Ar- $H$ ).  $^{13}\text{C}$  NMR (125.743 MHz, CDCl $_3$ ),  $\delta_C$  (TMS, ppm): 153.94, 138.08, 137.84, 134.79, 133.49, 132.62, 130.19, 129.92, 129.31, 128.15, 127.62, 127.38, 126.50, 125.57.  $^{29}\text{Si}$  NMR (99.3796 MHz, CDCl $_3$ ),  $\delta_{Si}$  (TMS, ppm): -43.21, -46.49. EMM-ESI-TOF-MS: m/z calcd. for [C $_{80}$ H $_{60}$ O $_4$ Si $_4$ +NH $_4$ ] $^+$ : 1214.3907; found 1214.3914.

### NMR spectra of Compounds 1-3

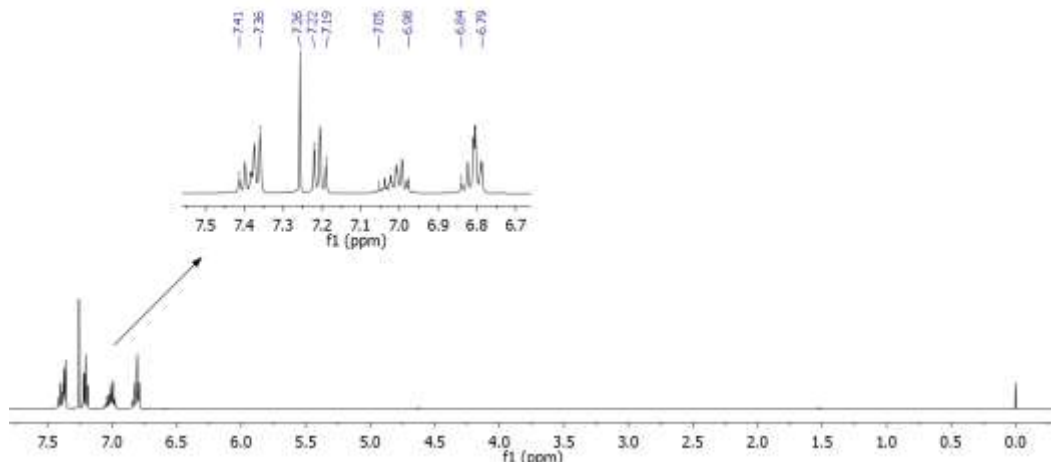


Figure S1.  $^1\text{H}$ -NMR of compound 1 (500.023 MHz, CDCl $_3$ /TMS)

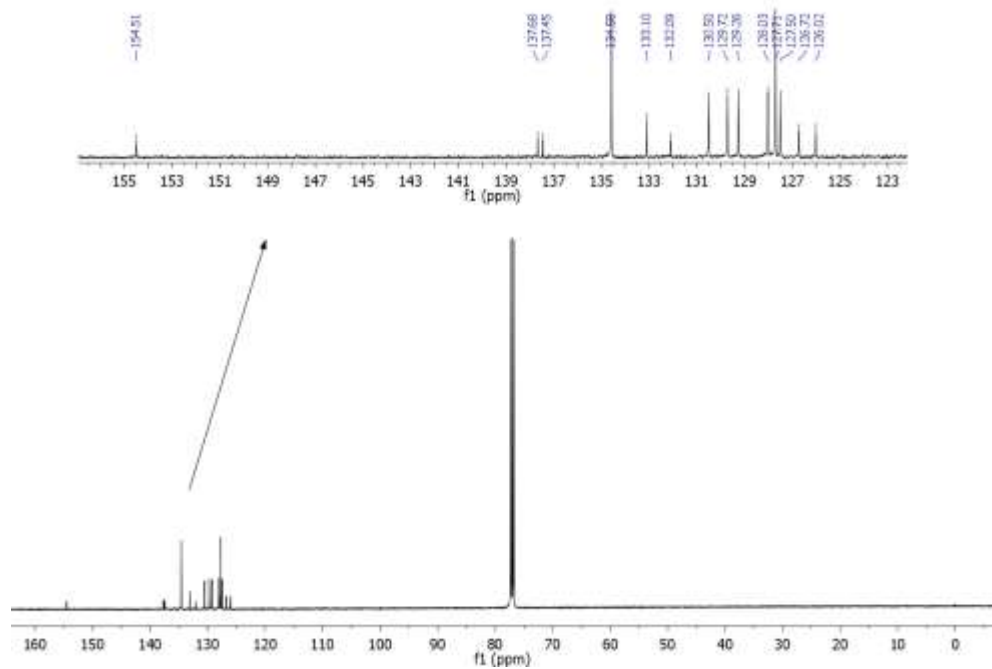


Figure S2.  $^{13}\text{C}$ -NMR of compound **1** (125.743 MHz,  $\text{CDCl}_3/\text{TMS}$ )

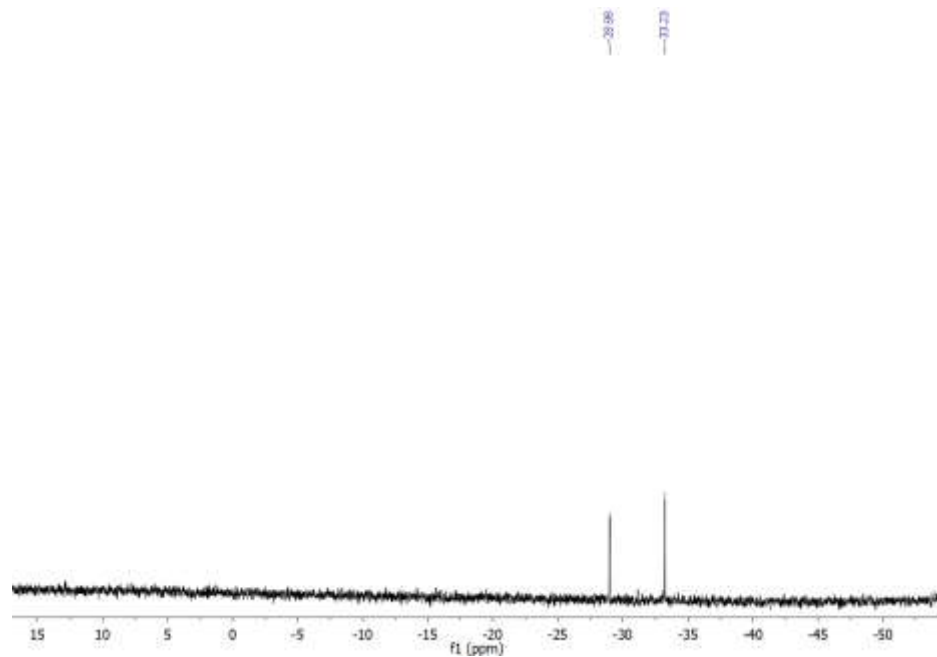


Figure S3.  $^{29}\text{Si}$ -NMR of compound **1** (99.3796 MHz,  $\text{CDCl}_3/\text{TMS}$ )

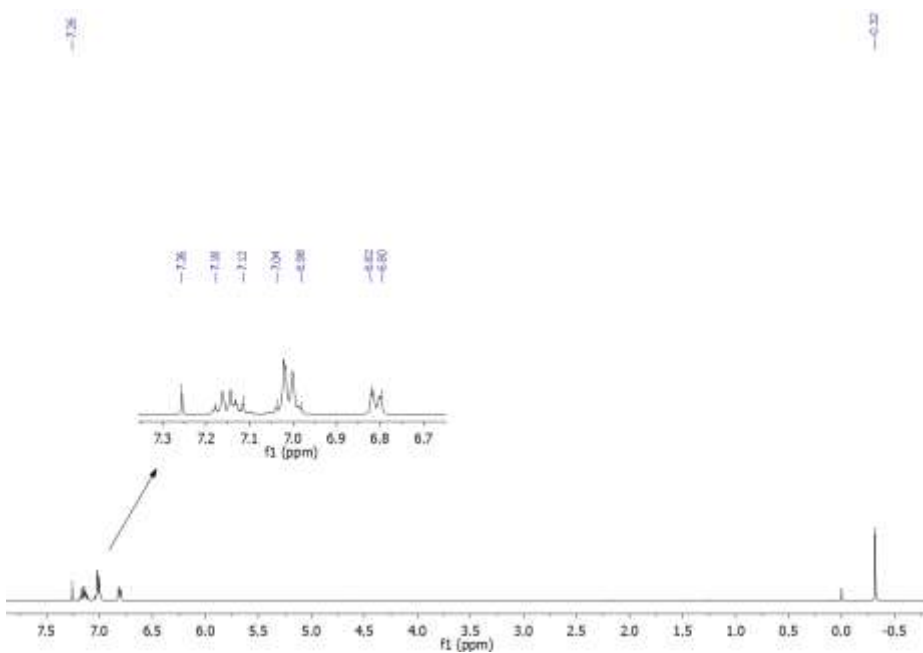


Figure S4. <sup>1</sup>H-NMR of compound 2 (400.182 MHz, CDCl<sub>3</sub>/TMS)

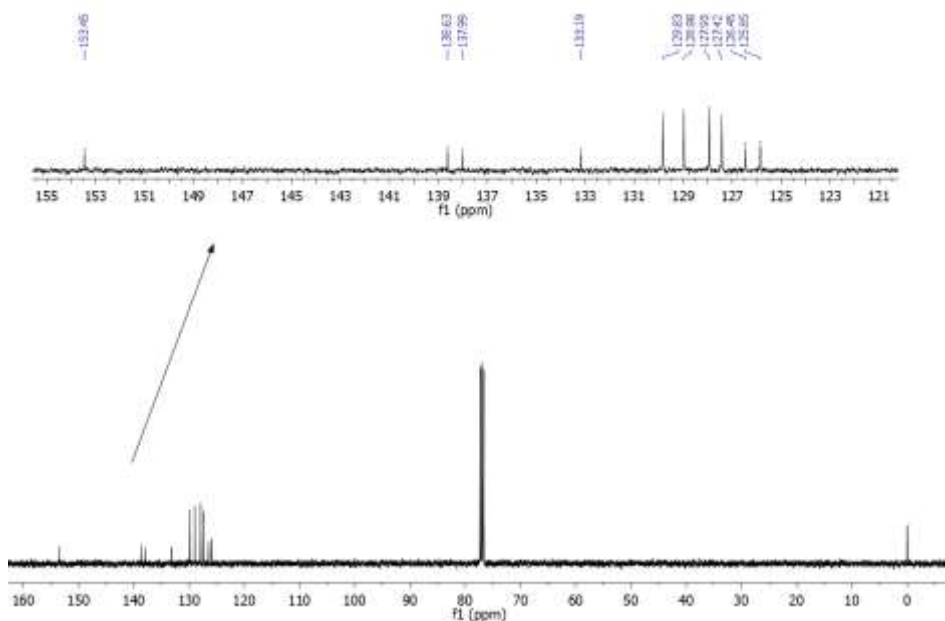


Figure S5. <sup>13</sup>C-NMR of compound 2 (100.635 MHz, CDCl<sub>3</sub>/TMS)

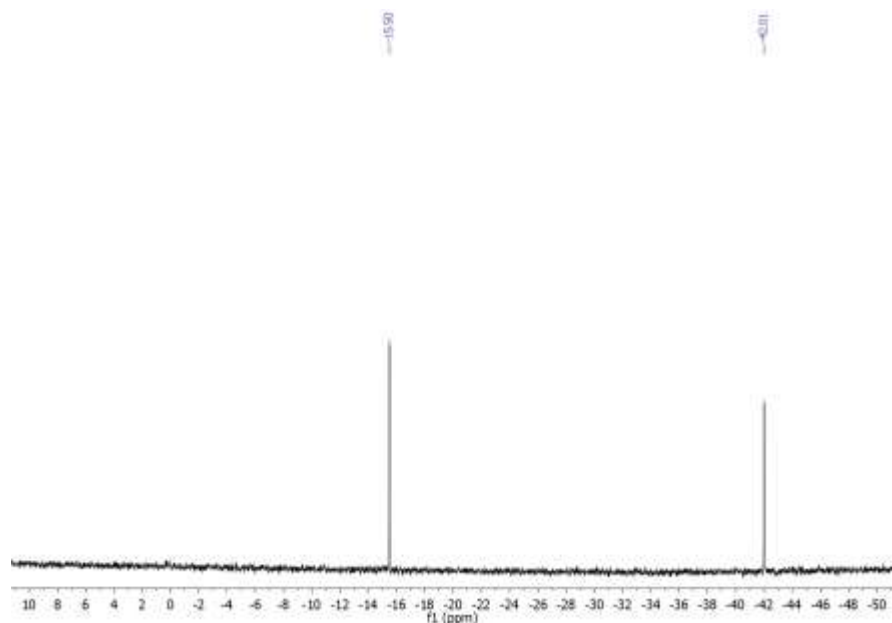


Figure S6.  $^{29}\text{Si}$ -NMR of compound 2 (99.3796 MHz,  $\text{CDCl}_3/\text{TMS}$ )

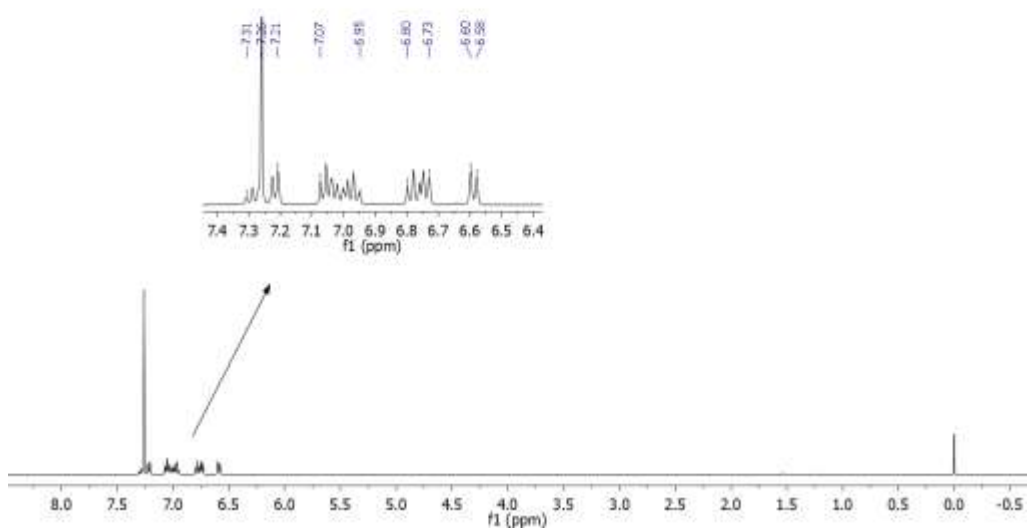


Figure S7.  $^1\text{H}$ -NMR of compound 3 (400.182 MHz,  $\text{CDCl}_3/\text{TMS}$ )

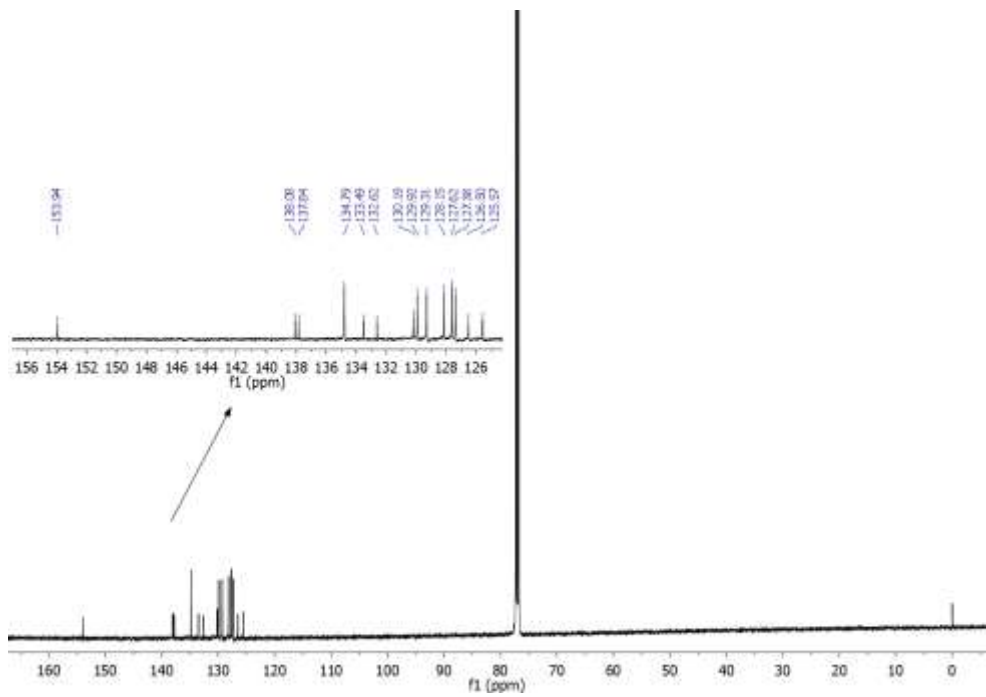


Figure S8.  $^{13}\text{C}$ -NMR of compound 3 (125.743 MHz,  $\text{CDCl}_3/\text{TMS}$ )

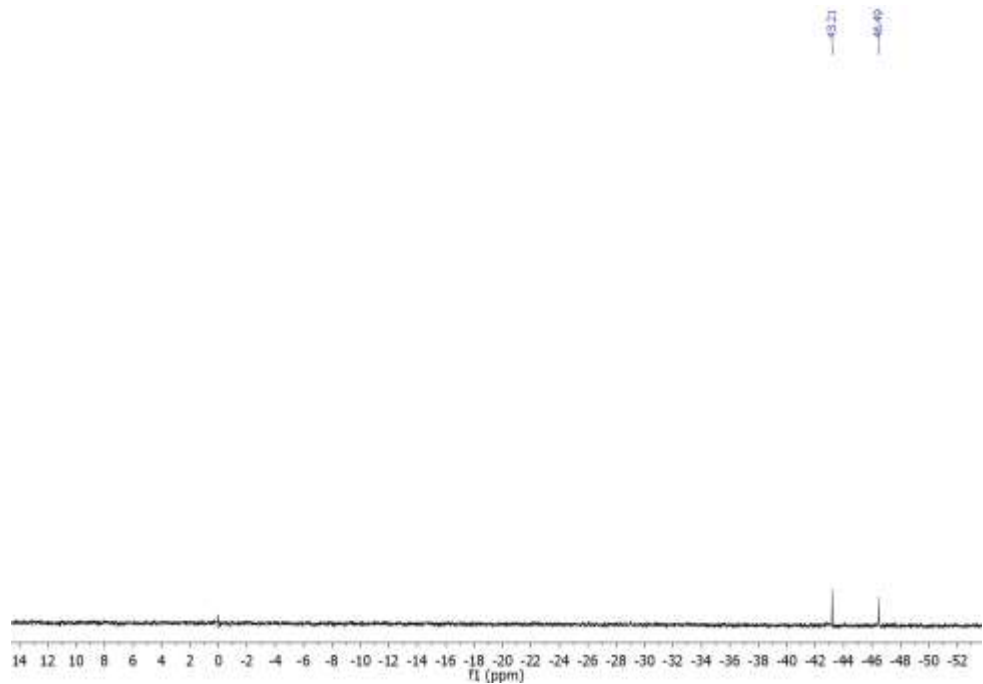


Figure S9.  $^{29}\text{Si}$ -NMR of compound 3 (99.3796 MHz,  $\text{CDCl}_3/\text{TMS}$ )

### Single Crystal X-ray Crystallography of Compounds 1-3

Table S1. The crystallographic details of compounds **1-3**, **S1** and **S2**.

	<b>1</b>	<b>2</b>	<b>3</b>	<b>S1<sup>[a]</sup></b>	<b>S2<sup>[b]</sup></b>
empirical formula	C <sub>52</sub> H <sub>40</sub> O <sub>3</sub> Si <sub>3</sub>	C <sub>60</sub> H <sub>52</sub> O <sub>4</sub> Si <sub>4</sub>	C <sub>80</sub> H <sub>60</sub> O <sub>4</sub> Si <sub>4</sub>	C <sub>60</sub> H <sub>52</sub> O <sub>4</sub> Si <sub>4</sub>	C <sub>28</sub> H <sub>22</sub>
formula weight	797.11	949.37	1197.64	949.37	358.45
crystal dimensions, mm	0.221 × 0.135 × 0.101	0.263 × 0.196 × 0.128	0.151 × 0.059 × 0.048	0.133 × 0.1 × 0.039	0.40 × 0.20 × 0.10
crystal system	triclinic	monoclinic	triclinic	triclinic	monoclinic
space group	<i>P</i> 1̄	C2/c	<i>P</i> 1̄	<i>P</i> 1̄	<i>P</i> 2 <sub>1</sub> /c
a/Å	10.688(4)	19.956(8)	11.226(3)	12.373(7)	7.860(3)
b/Å	14.471(8)	28.804(9)	12.704(3)	12.616(6)	5.7022(19)
c/Å	17.002(6)	10.023(3)	13.186(3)	18.679(7)	22.413(8)
α/°	104.62(5)	90	115.699(4)	75.714(15)	90
β/°	103.75(4)	102.117(6)	103.433(5)	73.48(2)	103.090(17)
γ/°	103.50(4)	90	101.434(5)	66.738(15)	90
Volume/Å <sup>3</sup>	2348.0(19)	5633(3)	1549.3(7)	2538(2)	978.5(6)
Z	2	4	1	2	2
ρ <sub>calc</sub> , mg/mm <sup>3</sup>	1.127	1.119	1.284	1.242	1.217
F(000)	836.0	2000.0	628.0	1000.0	380.0
λ/Å	Cu K $\alpha$ , 1.54178	Mo K $\alpha$ , 0.71073	Mo K $\alpha$ , 0.71073	Mo K $\alpha$ , 0.71073	Mo K $\alpha$ , 0.71073
μ/mm <sup>-1</sup>	1.237	0.149	0.150	0.165	0.069
temperature/K	100(1)	100(1)	100(1)	100(1)	100(1)
2θ range for data collection	5.66 to 144.838°	2.522 to 55.098°	3.674 to 53.17°	3.556 to 51.444°	3.732 to 63.522°
reflections collected	40264	65866	22893	25301	24189
independent reflections. (R <sub>int</sub> )	8905(0.0302)	6489(0.0294)	6424 (0.0512)	9643(0.0476)	3331(0.0305)
data/restraints/parameters	8905/673/641	6489/0/310	6424/0/397	9643/354/679	3331/0/127
goodness-of-fit on F <sup>2</sup>	1.040	1.038	1.019	1.016	1.060
R <sub>1,wR<sub>2</sub></sub> [I>=2σ (I)]	0.0385, 0.0984	0.0359, 0.1007	0.0442, 0.0952	0.0490, 0.1076	0.0453, 0.1309
R <sub>1,wR<sub>2</sub></sub> [all data]	0.0488, 0.1044	0.0416, 0.1056	0.0685, 0.1046	0.0792, 0.1197	0.0499, 0.1348
largest diff. peak/hole / e Å <sup>-3</sup>	0.36/-0.36	0.42/-0.29	0.37/-0.34	0.37/-0.32	0.50/-0.20

[a] A solvatomorph (**S1**) of compound **2**. [b] A polymorph of 1,2,3,4-tetraphenyl-1,3-butadiene (**S2**) was formed during the synthesis of cyclotetrasiloxanes if the reaction was carried out in the presence of Et<sub>2</sub>O.

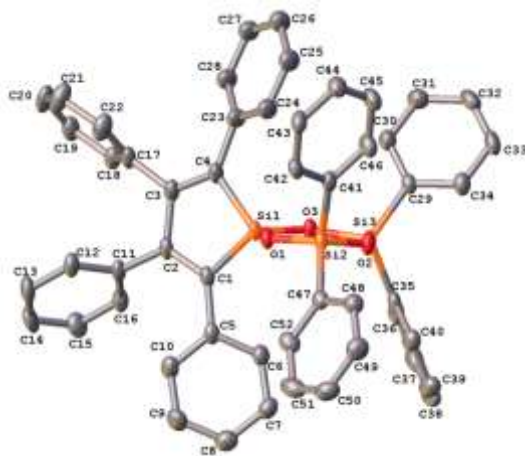


Figure S10. Thermal ellipsoids drawing of compound **1** (all H atoms are omitted)

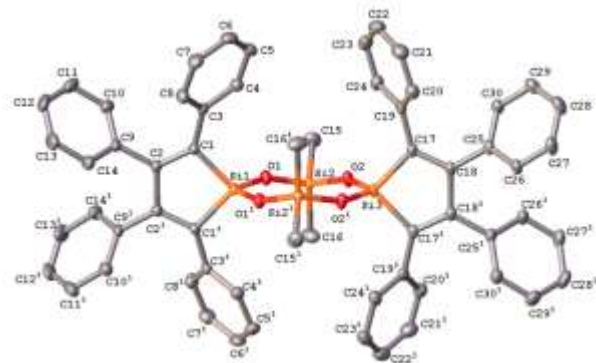


Figure S11. Thermal ellipsoids drawing of compound 2 (all H atoms are omitted)

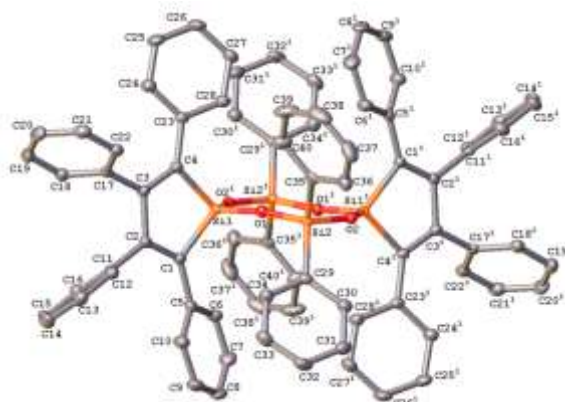


Figure S12. Thermal ellipsoids drawing of compound 3 (all H atoms are omitted)

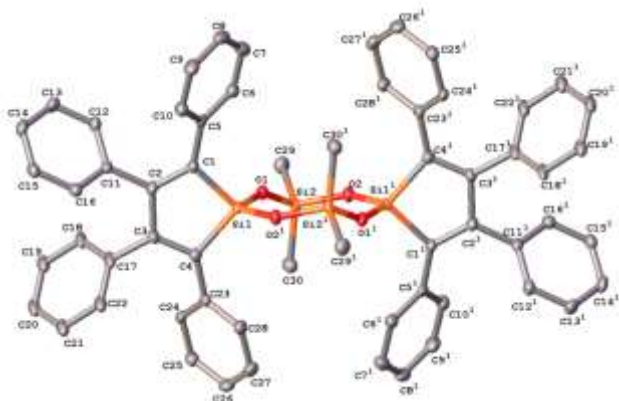


Figure S13. Thermal ellipsoids drawing of compound S1 (all H atoms are omitted)

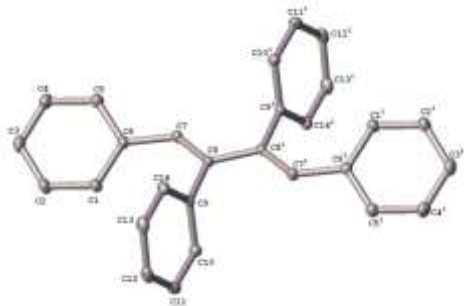


Figure S14. Thermal ellipsoids drawing of compound **S2** (all H atoms are omitted)

**Table S2.** Selected structural parameters of compounds **1-3**

	<b>1</b>	<b>2</b>	<b>3</b>
d(C–Si <sub>silole</sub> ) <sub>avg</sub> (Å)	1.855(3)	1.8516(4)	1.8565(15)
d(O–Si <sub>silole</sub> ) <sub>avg</sub> (Å)	1.634(2)	1.6132(3)	1.6168(11)
∠ (C–Si <sub>silole</sub> –C) (°)	94.3(2)	93.80(2)	94.77(9)
∠(O–Si <sub>silole</sub> –O) (°)	107.02(16)	109.79(2)	108.49(7)
cyclosiloxane ring planarity (RMSD)	0.041	0.136	0.052

The structural details of compounds **1-3** are highlighted in Table S2. The C-Si<sub>silole</sub> and O-Si<sub>silole</sub> bond lengths of these compounds are very similar to those found in silafluorene-containing compounds,<sup>[9]</sup> and these bond distances are within the range of those reported in the CSD for related silole and cyclosiloxane compounds.

Similarly, the C-Si<sub>silole</sub>-C and O-Si<sub>Ph-silole</sub>-O bond angles of **1-3** are within the range of those reported in the CSD for tetraphenylsilole (∠C-Si<sub>silole</sub>-C: 91°-95°) and cyclosiloxane structures. However, the C-Si<sub>silole</sub>-C bond angles (93.80°-94.77°) in **1-3** are all larger than those observed in the silafluorene-containing ring compounds (92.6°-93.43°).<sup>[9]</sup> We attribute the widening of the C-Si<sub>silole</sub>-C bond angle to the increased steric clash of the phenyl substituents on the silole group.

The degree of planarity of the cyclosiloxane ring was determined by fitting a plane to all Si and O atoms of the ring and measuring the root mean squared deviation (RMSD) of the atoms from that plane. In general, these cyclosiloxane rings are more nearly planar than those of the silafluorene-containing compounds.<sup>[9]</sup>

### Infrared Spectra of Compounds 1-3

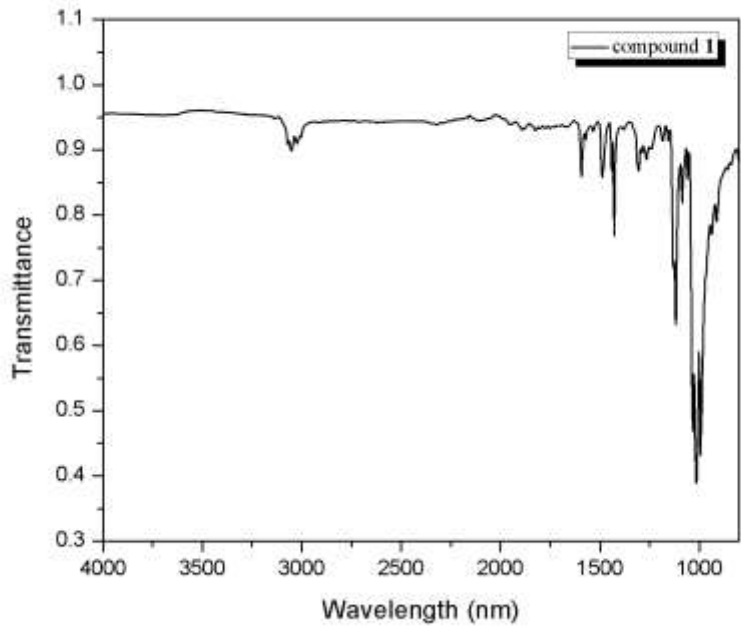


Figure S15. FTIR spectrum of compound 1.

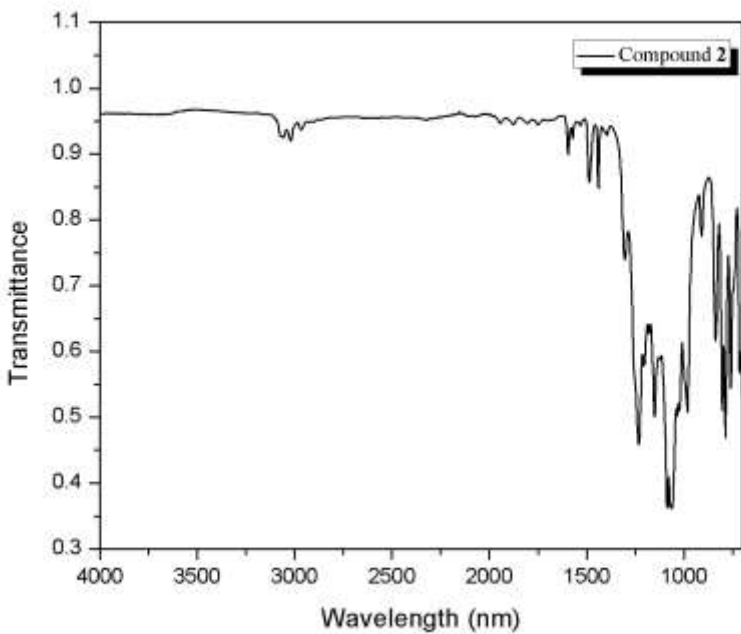


Figure S16. FTIR spectrum of compound 2.

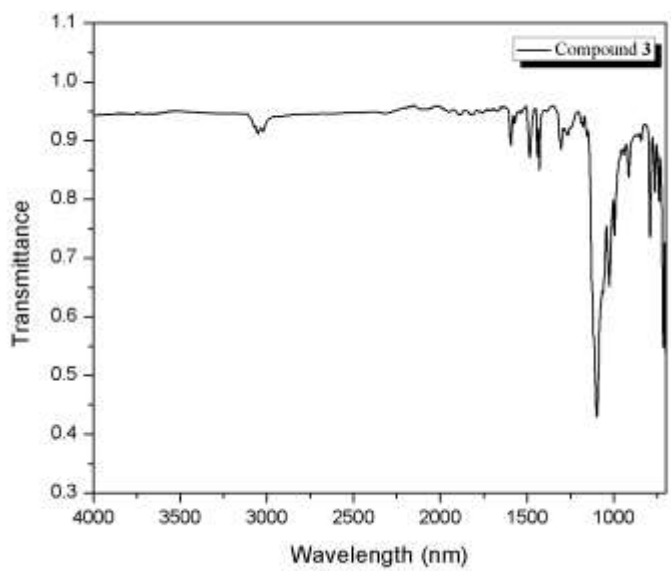


Figure S17. FTIR spectrum of compound **3**.

#### UV-Vis Absorption and Fluorescence Spectra of Compounds **1-3** in THF Solution and as crystals

Solutions of  $\sim$ 0.01 mg/ml compounds **1-3** in HPLC Grade THF were used to test the UV-Vis absorbance and fluorescence spectra at room temperature. Crystals of **1-3** were used to test the solid state fluorescence.

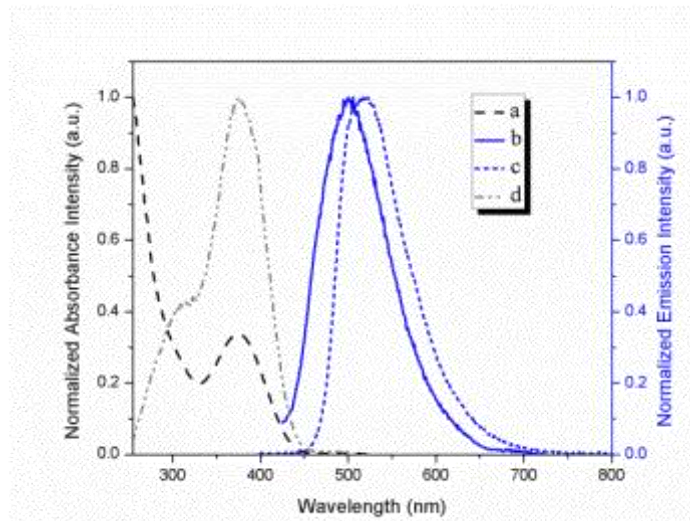


Figure S18. (a) Normalized UV absorption of **1** in THF solution; (b) Normalized fluorescence emission of **1** in THF solution,  $\lambda_{\text{ex}}=325$  nm; (c) Normalized fluorescence emission of **1** as crystals,  $\lambda_{\text{ex}}=325$  nm. (d) Fluorescence excitation spectrum of **1** in THF solution at  $\lambda_{\text{activation}}=500$  nm.

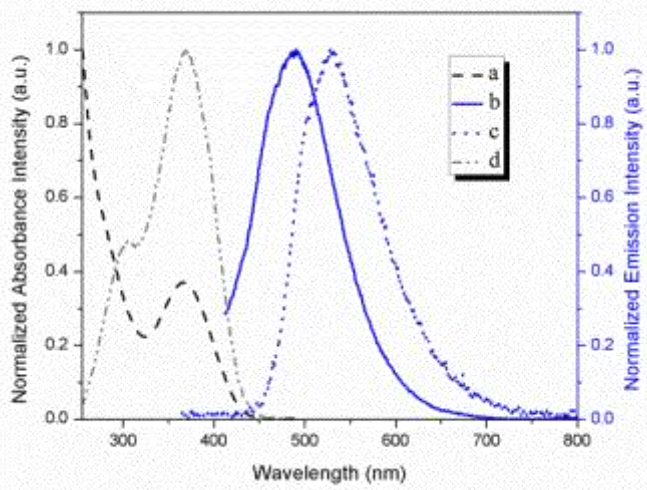


Figure S19. (a) Normalized UV absorption of **2** in THF solution; (b) Normalized fluorescence emission of **2** in THF solution,  $\lambda_{\text{ex}}=325$  nm; (c) Normalized fluorescence emission of **2** as crystals,  $\lambda_{\text{ex}}=325$  nm. (d) Fluorescence excitation spectrum of **2** in THF solution at  $\lambda_{\text{activation}}=490$  nm.

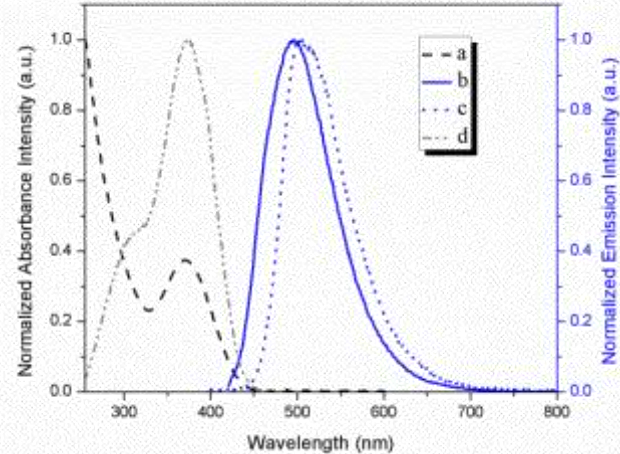


Figure S20. (a) Normalized UV absorption of **3** in THF solution; (b) Normalized fluorescence emission of **3** in THF solution,  $\lambda_{\text{ex}}=325$  nm; (c) Normalized fluorescence emission of **3** as crystals,  $\lambda_{\text{ex}}=325$  nm. (d) Fluorescence excitation spectrum of **3** in THF solution at  $\lambda_{\text{activation}}=496$  nm.

### Aggregation Enhanced Emission (AEE) of Compounds 2-3

Solutions of  $10^{-3}$  mg/ml compounds **1-3** in THF/H<sub>2</sub>O mixtures varying with 0-95% water content at room temperature were used to investigate the aggregation enhanced emission properties.

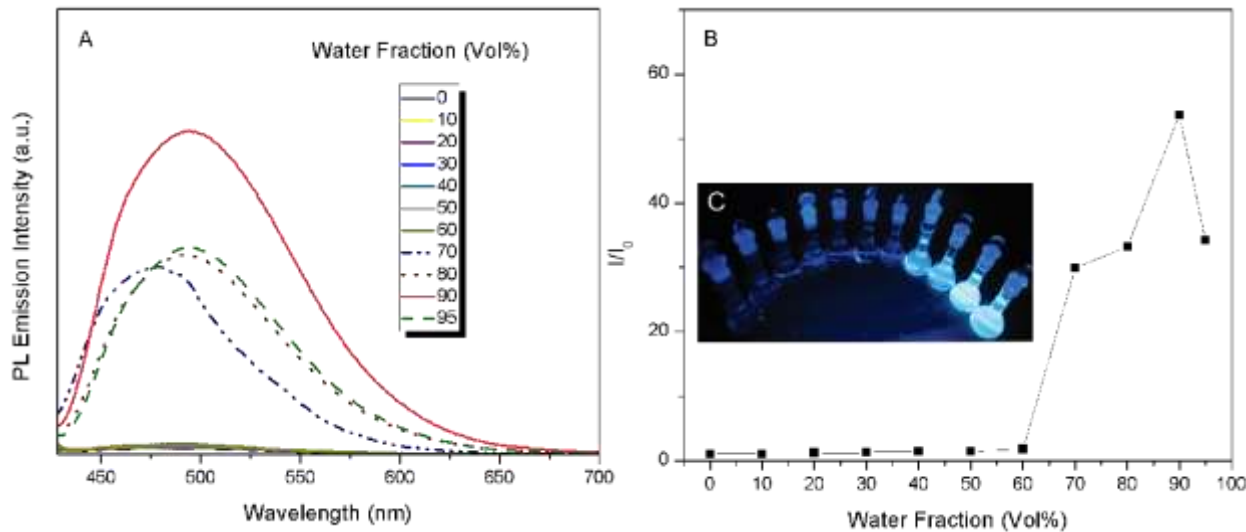


Figure S21. (A) PL Emission Spectra of  $10^{-3}$  mg/ml compound **2** in THF/H<sub>2</sub>O mixtures with different fractions of H<sub>2</sub>O. (B) Plot of  $I/I_0$  at 490 nm versus the water fraction, where  $I_0$  is the PL emission intensity in pure THF solution,  $\lambda_{ex}=370$  nm. (C) Photograph of **2** in THF/H<sub>2</sub>O mixtures containing different volume fractions of water taken under illumination of a UV lamp at 365 nm; from left to right: water fractions 0%-95%.

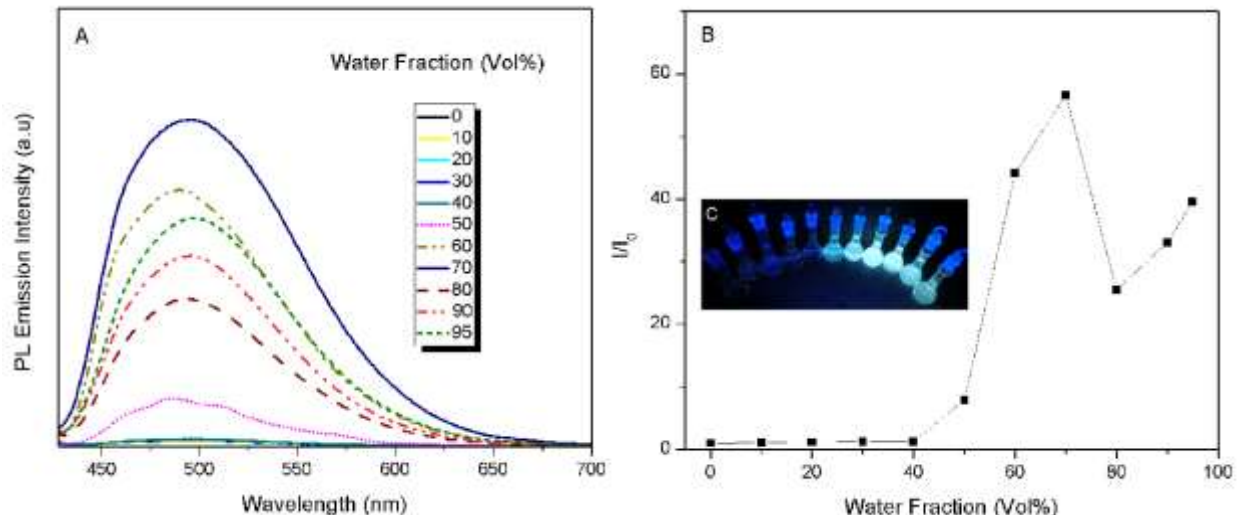


Figure S22. (A) PL Emission Spectra of  $10^{-3}$  mg/ml compound **3** in THF/H<sub>2</sub>O mixtures with different fractions of H<sub>2</sub>O. (B) Plot of  $I/I_0$  at 495 nm versus the water fraction, where  $I_0$  is the PL emission intensity in pure THF solution,  $\lambda_{ex}=370$  nm. (C) Photograph of **3** in THF/H<sub>2</sub>O mixtures containing different volume fractions of water taken under illumination of a UV lamp at 365 nm; from left to right: water fractions 0%-95%.

### Relative Fluorescence Quantum Yields of Compounds 1-3 in THF Solution

According to compounds **1-3**'s fluorescent emission in a similar region to Quinine sulfate, quinine sulfate dihydrate was chosen as a standard reference to measure the fluorescence quantum yield. To test fluorescence quantum yield, solutions of the standard and test samples with identical absorbance at the same excitation wavelength can be assumed to be absorbing the same number of photons, thus, a simple ratio of the integrated fluorescence intensities of the two solutions (recorded under identical conditions) will yield the ratio of the quantum yield values.<sup>[10]</sup>

Compared to a single-point method calculated using the integrated emission intensities from a single sample and standard reference pair at identical UV absorbance, calculating the slope of the linear fitting line generated by plotting the integrated fluorescence intensity against the absorption for multiple concentrations of fluorophores provides much higher accuracy. Hence, we use the following equation to determine the quantum yield.

$$\Phi_x = \Phi_{ST} \left( \frac{Grad_x}{Grad_{ST}} \right) \left( \frac{\eta_x^2}{\eta_{ST}^2} \right)$$

Where  $\Phi$  is the fluorescence quantum yield,  $Grad$  is the gradient of the linear fitting line from the plot of integrated fluorescence intensity vs absorbance,  $\eta$  is the refractive index of the solvent, the subscripts X and ST denote standard and test sample respectively.

In this study, quantum yields of compounds **1-3** were investigated in HPLC Grade THF using quinine sulfate in 0.1N H<sub>2</sub>SO<sub>4</sub> as a standard. All measurements were carried out at room temperature. The UV-Vis absorbance in the studied range (350-650nm) was kept below 0.1 using 10mm path length 23-Q-10 Starna Quartz Cells to avoid re-absorption effects.<sup>[11]</sup> The fluorescence intensity was kept below  $3 \times 10^6$  according to the limitation of the detector and acquisition of better signal to noise ratio. The quantum yield of quinine sulfate in 0.1N H<sub>2</sub>SO<sub>4</sub> reported is 0.577<sup>[12]</sup> under excitation wavelength 350 nm. The refractive indexes of THF and 0.1N H<sub>2</sub>SO<sub>4</sub> at room temperature are 1.406 and 1.33, respectively. The following parameters were used for the acquisition of fluorescence data.

Fluorescence Emission mode:

Activate: 350nm, Slit: 1.2nm

Start: 360nm, End: 700nm, Inc: 1, Slit: 1 nm

After subtracting background fluorescence, the integrated fluorescence intensities of all samples were calculated from 370 nm to 650nm.

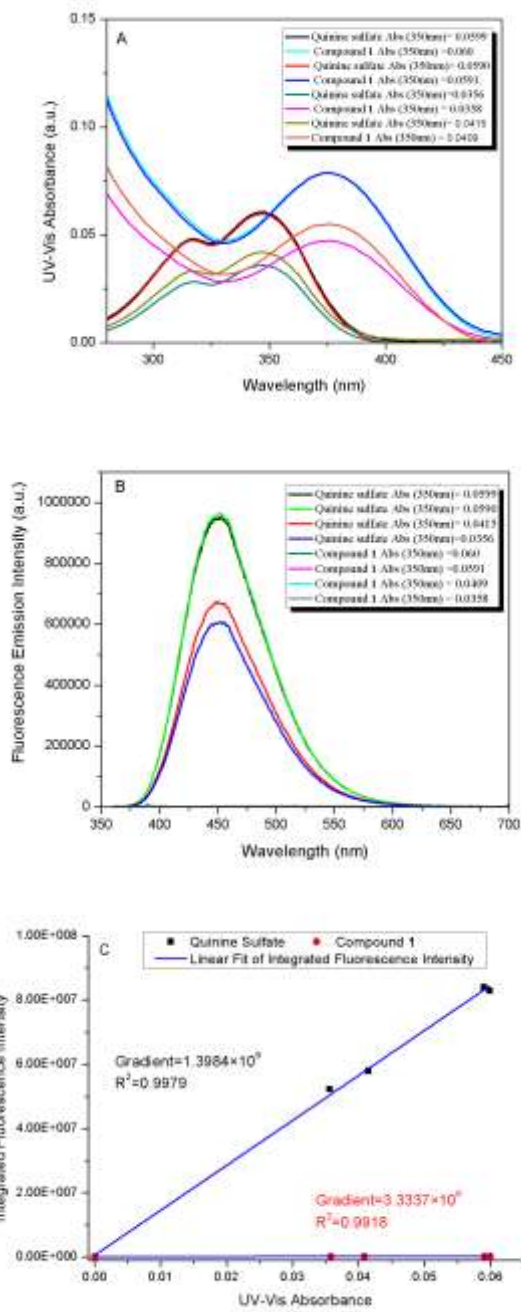


Figure S23. (A) UV-Vis Absorbance Cross Point of quinine sulfate and compound **1** at 350 nm. (B) Fluorescence Emission Intensity of quinine sulfate and compound **1** at  $\lambda_{\text{ex}} = 350\text{nm}$ . (C) Linear Fit of Integrated Fluorescence Intensity of quinine sulfate and compound **1**.

$$\Phi(1)_{\text{THF solution}} = 0.577 \left( \frac{3.3337 \times 10^6}{1.3984 \times 10^9} \right) \left( \frac{1.406}{1.33} \right)^2 = 0.0015$$

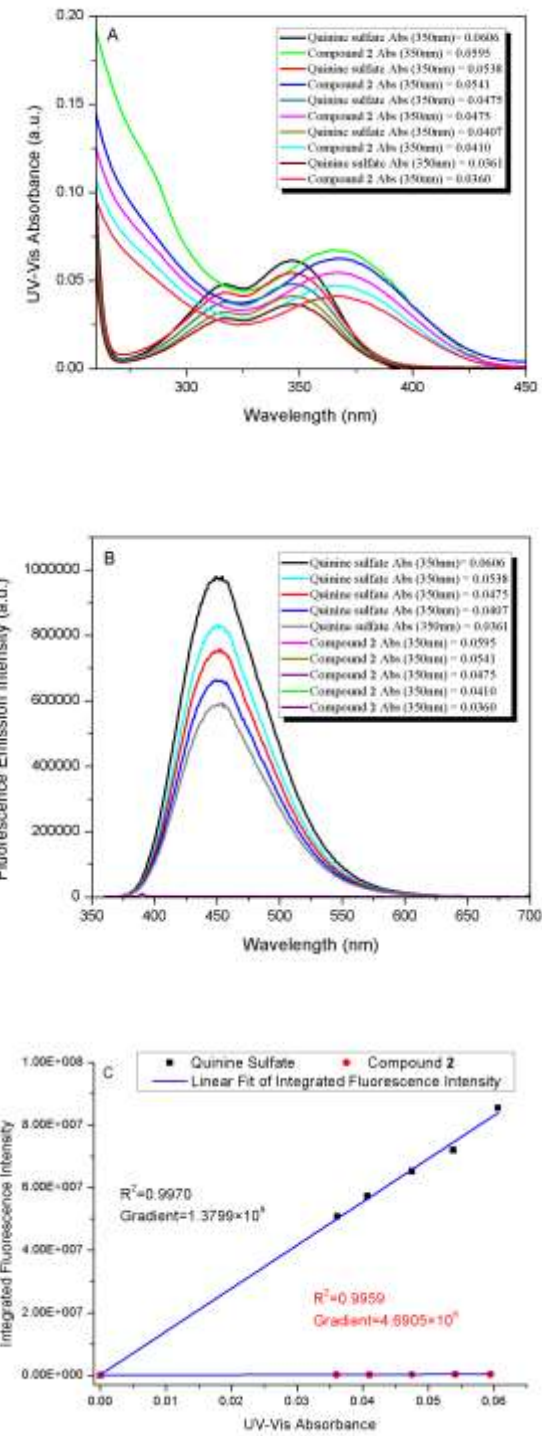


Figure S24. (A) UV-Vis Absorbance Cross Point of quinine sulfate and compound **2** at 350 nm. (B) Fluorescence Emission Intensity of quinine sulfate and compound **2** at  $\lambda_{\text{ex}}=350\text{nm}$ . (C) Linear Fit of Integrated Fluorescence Intensity of quinine sulfate and compound **2**.

$$\Phi(2)_{\text{THF solution}} = 0.577 \left( \frac{4.6905 \times 10^6}{1.3799 \times 10^9} \right) \left( \frac{1.406}{1.33} \right)^2 = 0.0022$$

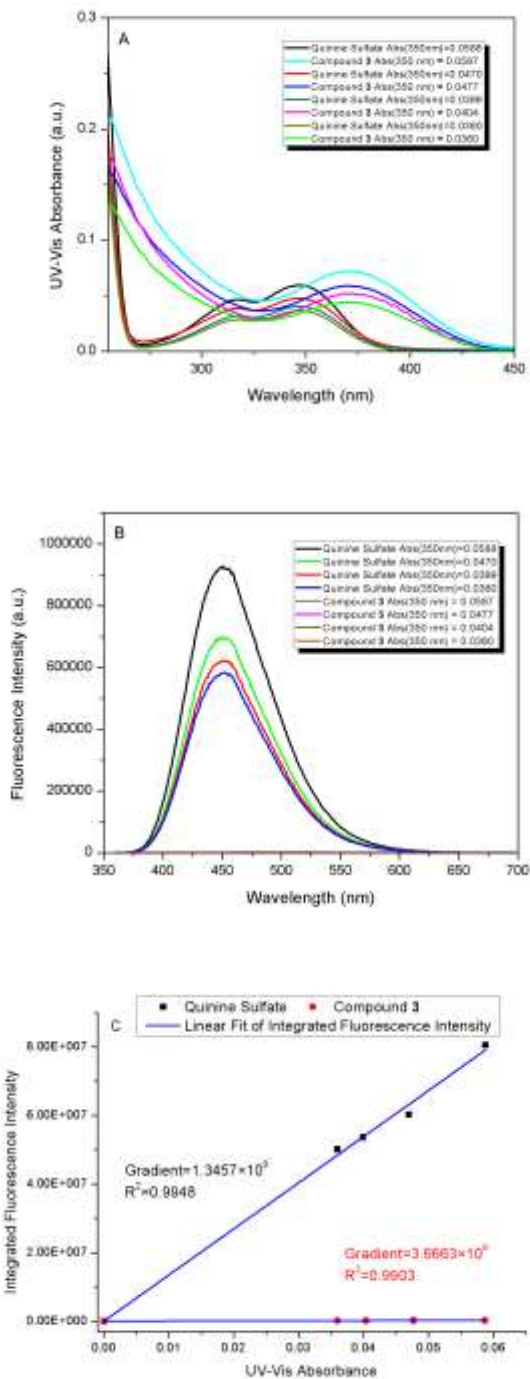


Figure S25. (A) UV-Vis Absorbance Cross Point of quinine sulfate and compound **3** at 350 nm. (B) Fluorescence Emission Intensity of quinine sulfate and compound **3** at  $\lambda_{ex}=350\text{nm}$ . (C) Linear Fit of Integrated Fluorescence Intensity of quinine sulfate and compound **3**.

$$\Phi(3)_{\text{THF solution}} = 0.577 \left( \frac{3.6663 \times 10^6}{1.3457 \times 10^3} \right) \left( \frac{1.406}{1.33} \right)^2 = 0.0018$$

### Absolute Solid State Fluorescence Quantum Yield of Compounds 1-3

The absolute solid state fluorescence quantum yields of compounds **1-3** were determined on a calibrated integrating sphere according to the method described by de Mello et al.,<sup>[3]</sup> using a 325nm CW light from a He-Cd laser for optical pumping, an Ocean Optics USB2000 miniature fiber optics spectrometer and the same procedure reported elsewhere.<sup>[4]</sup> The solid state quantum yield is calculated by the number of photons emitted divided by the number of photons absorbed. The calculation of the number of photons (the integration of the spectral peaks, see Figures S18-S20) was carried out through Matlab.

### Interactions of **1-3** in the unit cell

The CH- $\pi$  interaction is a weak non-covalent interaction (~4.2 KJ/mol) in which an aliphatic or aromatic CH bond interacts with the  $\pi$ -face of an aromatic system.<sup>[13]</sup> We consider CH- $\pi$  interactions with distance smaller than 2.9 Å (the expected van der Waals distance of CH- $\pi$  interaction distance).<sup>[13,14]</sup> A typical  $\pi$ - $\pi$  interaction (~2 KJ/mol)<sup>[15]</sup> is a non-covalent interaction between aromatic groups with the distance smaller than 3.8 Å.

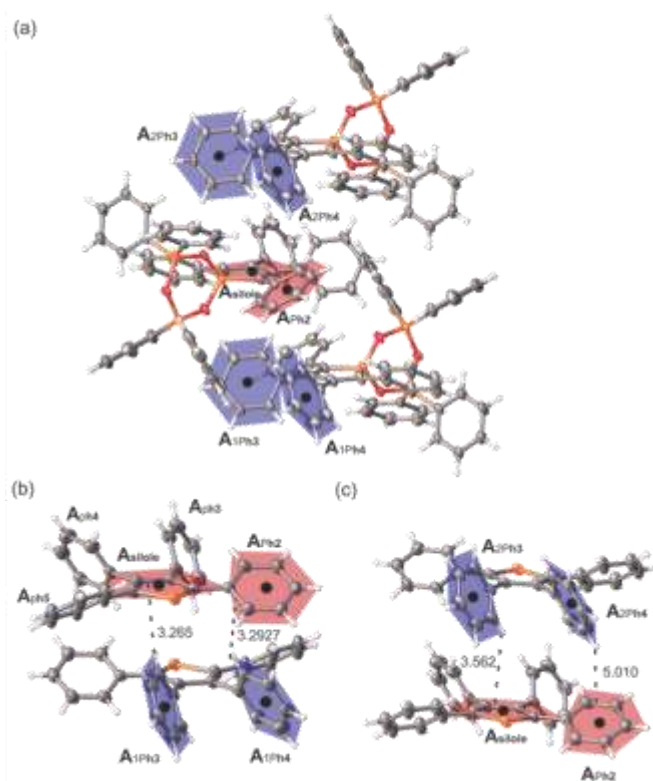


Figure S26. Intermolecular C-H $\cdots$  $\pi$  interactions of tetraphenylsilole in compound **1** in solid state (powder). (a) A segment of the unit cell of **1** as taken from the X-ray structure showing interactions for one type of tetraphenylsilole moieties A. For clarity only planes of interacting tetraphenylsilole moieties (highlighted in red or blue) are shown. (b) (c) intermolecular interactions of tetraphenylsilole moiety A. All distances are in Å.

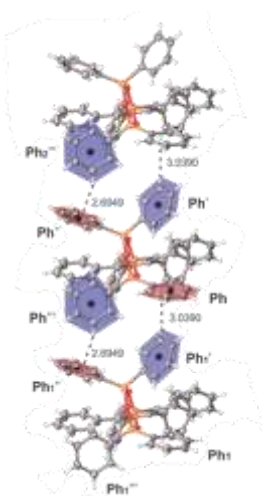


Figure S27. Intermolecular C-H $\cdots$  $\pi$  interactions of phenyls in compound **1** in solid state (powder). A segment of the unit cell of **1** as taken from the X-ray structure showing interactions between two types of phenyl moieties  $\text{Ph}_1''$  and  $\text{Ph}'''$ . For clarity only planes of interacting tetraphenylsilole moieties (highlighted in red or blue) are shown. All distances are in Å.

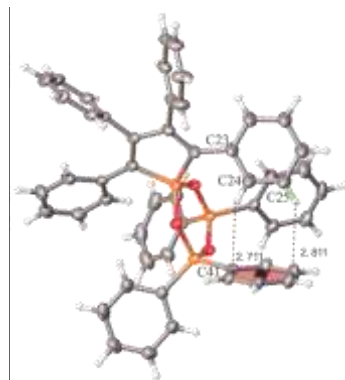


Figure S28. Intramolecular C-H $\cdots$  $\pi$  interactions in compound **1**. All distances are in Å.

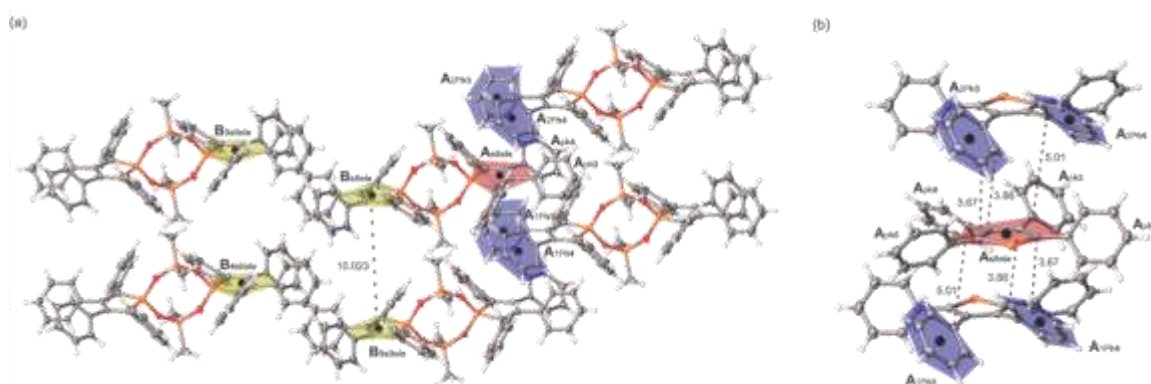


Figure S29. Intermolecular interactions of tetraphenylsilole in compound **2** in solid state (powder). (a) A segment of the unit cell of **2** as taken from the X-ray structure showing interactions for two types of tetraphenylsilole moieties A and B. For clarity only planes of interacting tetraphenylsilole moieties (highlighted in red, yellow or blue) are shown. (b) intermolecular interactions of tetraphenylsilole moiety A. All distances are in Å.

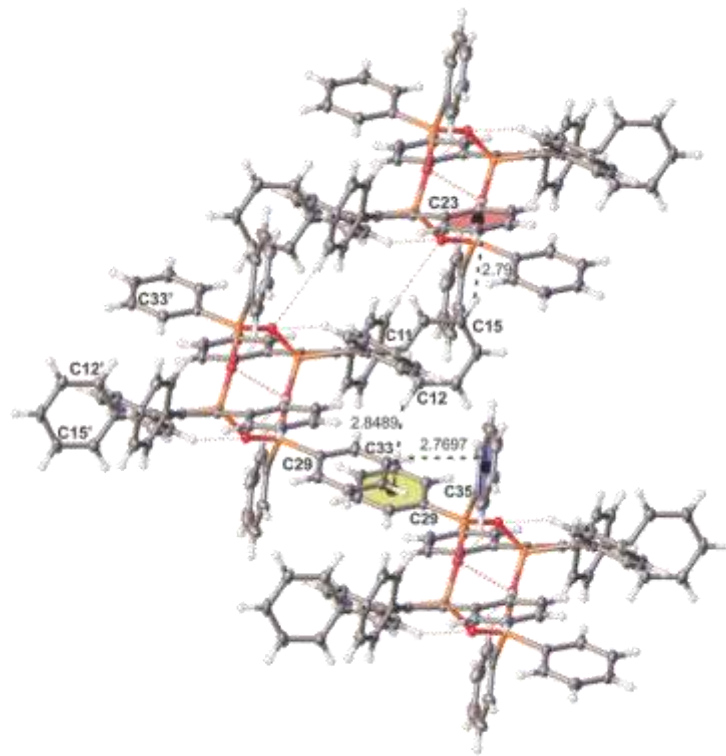


Figure S30. Intermolecular C-H $\cdots$  $\pi$  interactions in compound **3**. A segment of the unit cell of **3** as taken from the X-ray structure showing interactions between phenyl rings C11 and C23 (distance 2.7921), C11 and C29 (distance 2.8489), C29 and C35 (distance 2.7697). For clarity only planes of interacting phenyls (highlighted in red, yellow and blue) are shown. All distances are in Å.

### Excited State UV-Vis Calculations and Molecular Orbitals of **1-3**

**Table S3.** Excitation energies (given as wavelengths  $\lambda$  in [nm]) and oscillator strengths (in brackets) are given for the five energetically lowest-lying excited states of **1-3** (single molecule) as calculated by TD-DFT/ B3LYP/6-31G (d).

	<b>1</b>			<b>2</b>			<b>3</b>		
	transitions	E <sup>[a]</sup>	$\lambda_{\text{ex}}$ (osc)	transitions	E <sup>[a]</sup>	$\lambda_{\text{ex}}$ (osc)	transitions	E <sup>[a]</sup>	$\lambda_{\text{ex}}$ (osc)
S <sub>1</sub> <sup>[b]</sup>	HOMO $\rightarrow$ LUMO	1.97	630 (0.29)	HOMO $\rightarrow$ LUMO	1.97	630 (0.32)	HOMO $\rightarrow$ LUMO	1.94	639 (0.32)
S <sub>2</sub> <sup>[b]</sup>	HOMO-1 $\rightarrow$ LUMO	2.96	419 (0.21)	HOMO $\rightarrow$ LUMO	2.52	493 (0.00)	HOMO $\rightarrow$ LUMO	2.45	507 (0.00)
S <sub>3</sub> <sup>[b]</sup>	HOMO-2, HOMO-4 $\rightarrow$ LUMO	3.36	370 (0.02)	HOMO $\rightarrow$ LUMO+1	2.65	468 (0.00)	HOMO $\rightarrow$ LUMO+1	2.63	471 (0.00)
S <sub>4</sub> <sup>[b]</sup>	HOMO-3, HOMO-5 $\rightarrow$ LUMO	3.45	359 (0.06)	HOMO $\rightarrow$ LUMO+1	2.89	429 (0.36)	HOMO $\rightarrow$ LUMO+1	2.84	437 (0.35)
S <sub>5</sub> <sup>[b]</sup>	HOMO-2, HOMO-4, HOMO-5 $\rightarrow$ LUMO	3.47	357 (0.00)	HOMO-1 $\rightarrow$ LUMO	3.03	409 (0.20)	HOMO-1 $\rightarrow$ LUMO	3.00	413 (0.20)

[a] Excitation energy given in eV; [b] excited states.

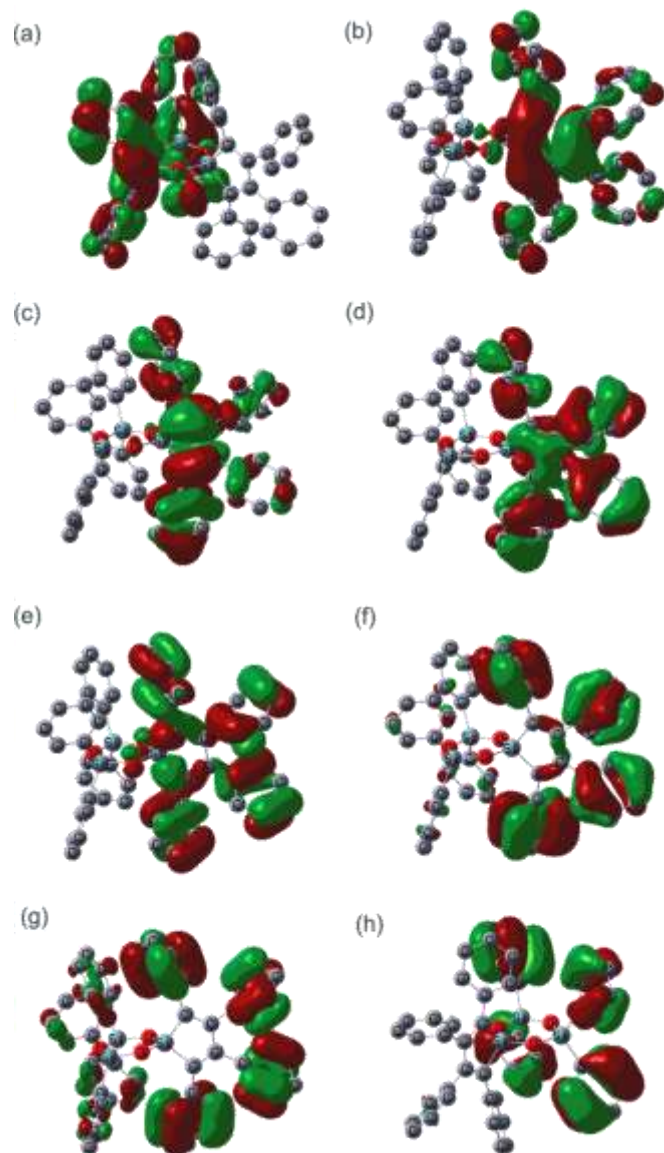


Figure S31. (a) LUMO+1; (b) LUMO; (c) HOMO; (d) HOMO-1; (e) HOMO-2; (f) HOMO-3; (g) HOMO-4; (h) HOMO-5 in compound **1**.

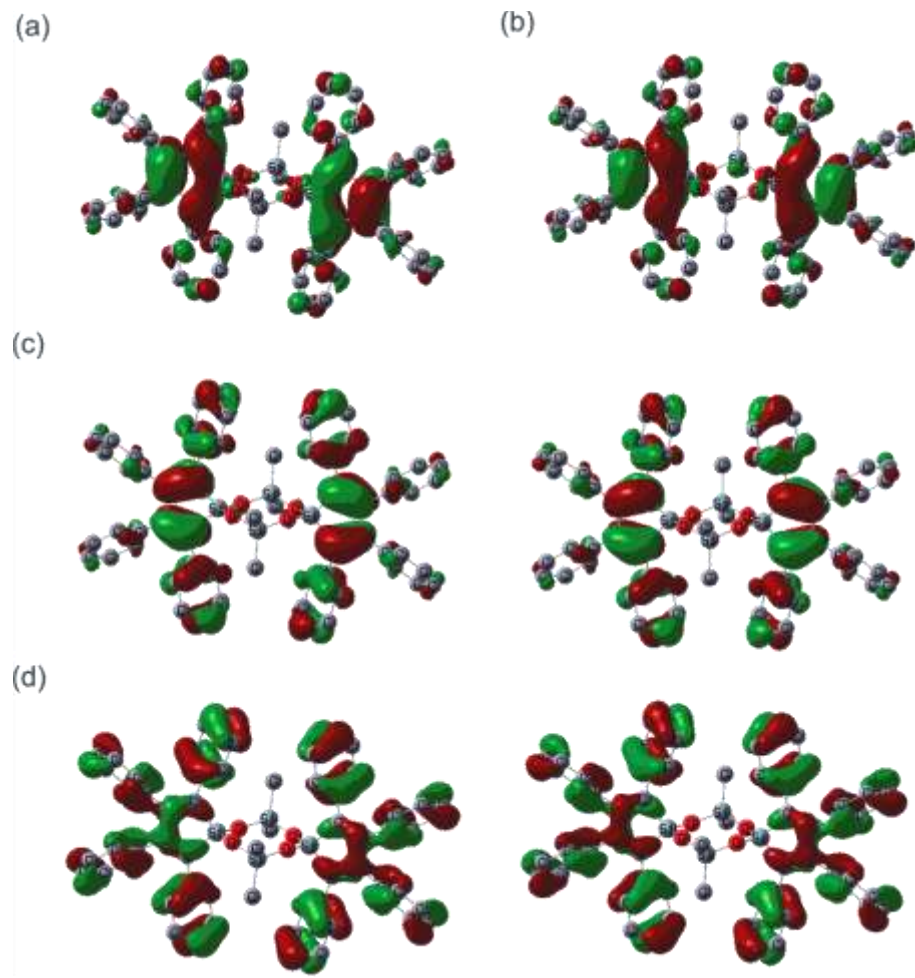


Figure S32. (a) LUMO+1; (b) LUMO; (c) HOMO; (d) HOMO-1 in compound 2.

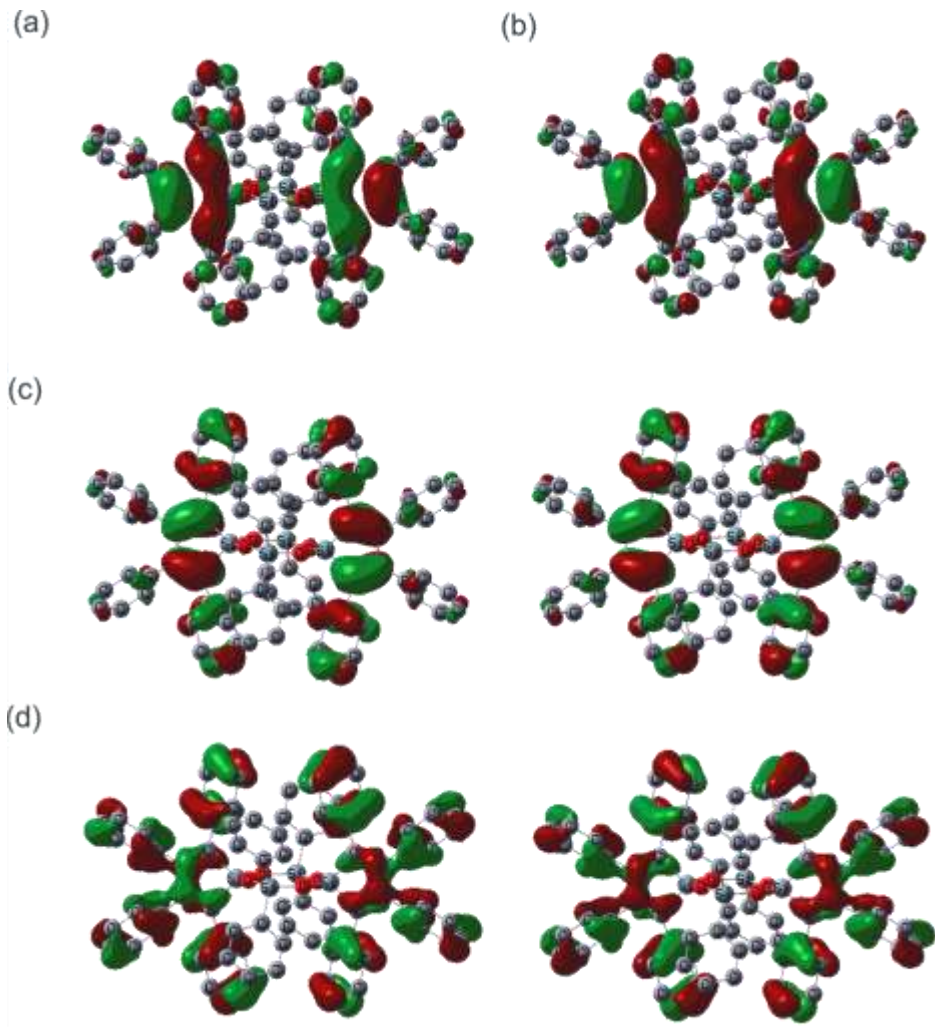


Figure S33. (a) LUMO+1; (b) LUMO; (c) HOMO; (d) HOMO-1 in compound 3.

## Optimized Geometry of Compounds 1-3 (single molecule)

The nature of stationary points on the PES (potential energy surface) was determined by calculations of full Hessian matrix followed by frequency calculations. All structures reported were found to be true minima on the PSE with no negative frequencies.

Table S4. Optimized geometry of compound **1** (single molecule) at B3LYP/6-31G (d).

Atom number	x	y	z
14	0.469151	0.000175	-0.000096
8	-0.520187	0.166349	1.326049
14	-2.180872	0.153421	1.525139
8	-2.836084	-0.000331	0.000172
14	-2.181057	-0.153739	-1.524896
8	-0.520323	-0.165891	-1.326139
6	-2.684417	-1.768821	-2.319912
6	-1.843778	-2.897495	-2.291281
1	-0.862739	-2.829628	-1.829911
6	-2.247547	-4.110353	-2.851148
1	-1.581684	-4.968537	-2.818926
6	-3.502378	-4.218162	-3.456952
1	-3.817035	-5.161556	-3.895652
6	-4.351262	-3.109236	-3.499303
1	-5.326969	-3.180709	-3.971748
6	-3.943436	-1.889038	-2.938123
1	-4.612748	-1.042126	-2.990395
6	-2.728013	1.333712	-2.540136
6	-2.300119	1.320042	-3.938631
1	-2.141173	0.042605	-4.442800
6	-2.933634	2.43832	-4.700636
1	-5.795420	2.427630	-5.778549
6	-3.488210	3.559327	-4.076790
1	-3.782279	4.422148	-4.668737
6	-3.668621	3.566171	-2.691562
1	-4.106502	4.432887	-2.203296
6	-3.291479	2.456096	-1.932441
1	-3.439318	2.473443	-0.855963
6	-2.727058	-1.318858	-2.540628
6	-2.559290	-1.330963	-3.938942
1	-2.139248	-0.463216	-4.442965
6	-2.931379	-2.439541	-4.701046
1	-2.792577	-2.428426	-5.778884
6	-3.486176	-3.560038	-4.077398
1	-3.779831	-4.422944	-4.669424
6	-3.667334	-3.566775	-2.692267
1	-4.105385	-4.433494	-2.204159
6	-3.290724	-2.446589	-1.933043
1	-3.439145	-2.473842	-0.856644
6	-2.684793	1.768359	-2.320094
6	-3.943172	1.896741	-2.939769
1	-6.611616	1.040234	-2.993312
6	-4.351440	3.107865	-3.500796
1	-5.326637	3.184980	-3.974399
6	-3.503650	4.217559	-3.456802
1	-3.818648	5.160899	-3.895374
6	-2.249454	4.110593	-2.851518
1	-1.584431	4.969375	-2.816018
6	-1.845242	2.897806	-2.289822
1	-0.864697	2.830602	-1.827301
6	1.745532	1.364809	-0.117736
6	2.965510	0.761564	-0.047629
6	2.965554	-0.761042	0.047517
6	1.745614	-1.364390	0.117486
6	1.445761	-2.810815	0.114876
6	0.442062	-3.311804	0.966994
1	-0.066352	-2.633971	1.646603
6	0.101699	-4.664531	0.963382
1	-0.673071	-5.022916	1.635850
6	0.743974	-5.547966	0.093240
1	0.475970	-6.601012	0.083904
6	1.730271	-5.604367	-0.771837
1	2.229010	-5.740905	-1.461130
6	2.079237	-3.714473	-0.761061
1	2.839921	-3.350035	-1.443766
6	4.258058	-1.504092	0.067763
6	5.171446	-1.486044	-1.830512
1	4.947952	-0.764446	-1.839818
6	6.364256	-2.133215	-0.975125
1	6.665899	-2.052519	-1.809488
6	6.669325	-2.570734	0.111180
1	7.600283	-3.517231	0.127530
6	5.771728	-3.054021	1.176866
1	6.001616	-3.689164	2.028213
6	4.574710	-2.337784	1.153629
1	3.876726	-2.419158	1.980822
6	4.257966	1.504700	-0.067770
6	5.173257	1.407366	0.993596
1	4.947729	0.765129	1.839891
6	6.364028	2.133966	0.975309
1	7.055595	2.053324	1.809738
6	6.669150	2.957783	-0.110981
1	7.600078	3.518024	-0.127255
6	5.771648	3.054701	-1.176754
1	6.001580	3.689844	-2.028090
6	4.574671	2.338391	-1.152621
1	3.876763	2.419708	-1.980882
6	1.445519	2.811201	-0.115306
6	0.441832	3.311967	-0.967575
1	-0.066440	2.633987	-1.647146
6	0.101301	4.664655	-0.964147
1	-0.673456	5.022869	-1.636723
6	0.743394	5.548269	-0.094052
1	0.475262	6.601284	-0.084861
6	1.729678	5.064891	0.771164
1	2.228273	5.741569	1.460424
6	2.078810	3.715039	0.760576
1	2.839474	3.350772	1.443396

Table S5. Optimized geometry of compound **2** (single molecule) at B3LYP/6-31G (d).

Atom number	x	y	z
14	-2.298137	0.008440	-0.017330
8	-1.355942	0.085099	1.611111
14	-0.015983	-0.5590913	2.164033
8	1.352055	-0.009763	1.361679
14	2.298136	-0.008469	0.017324
8	1.355835	0.068168	-1.330411
14	0.015881	0.596871	-2.164041
8	-1.352048	0.090711	-1.361678
6	0.028062	-0.244385	-3.833914
1	0.001117	-1.355332	-3.729373
6	0.849694	0.044582	-0.254602
1	0.922650	0.031961	-4.405901
6	0.030575	2.463664	-2.282263
1	0.929393	2.813833	-2.803365
1	-0.844653	2.824286	-2.834864
1	0.015330	2.930414	-1.291464
6	3.585370	-1.370647	-0.069253
6	4.005350	-0.000000	-0.069253
6	0.798460	0.761070	0.038072
6	3.576853	1.361321	0.101285
6	3.289792	2.810569	0.099778
6	2.331722	3.330330	0.991853
1	1.837661	2.657674	1.687724
6	2.029677	4.692302	1.009864
1	1.303099	5.072400	1.723668
6	0.555730	5.524021	1.162552
1	2.414864	6.623350	0.123979
6	3.589584	5.059918	-0.793082
1	4.074403	5.726803	-1.501465
6	3.906067	3.702109	-0.799625
1	4.631955	3.322141	-1.511380
6	6.089596	1.508748	0.046979
6	6.620101	1.441645	-1.002121
1	8.768248	0.755180	-1.862742
6	8.188236	2.138635	-1.011562
1	8.874477	2.056474	-1.850294
6	8.499377	2.966170	0.7070181
1	9.429465	3.528018	0.078677
6	7.608555	3.064650	1.141332
1	7.842801	3.702896	1.989231
6	6.613588	2.888589	1.270999
1	5.720115	2.428912	1.959445
6	6.100425	1.497796	-0.058607
6	7.026422	1.390458	0.992345
1	6.805572	-0.746064	1.838320
6	8.222267	-2.108479	0.964309
1	8.922158	-2.019445	1.790974
6	8.521718	-2.934790	-0.121678
1	8.450770	-3.408226	-0.145578
6	7.433887	3.032379	-1.177169
1	7.838359	-3.679706	-2.028188
6	6.411903	-2.333717	-1.143101
1	5.705380	-2.423861	-1.963171
6	3.307423	-2.821289	-0.045552
6	2.316944	-3.354991	-0.893033
1	1.795854	-0.926016	-1.576926
6	2.168259	-4.717777	0.832119
1	2.161970	5.107975	-1.557772
6	2.682836	-5.577157	-0.004685
1	2.444826	-6.637273	0.010059
6	3.651036	-5.059708	0.860147
1	4.165981	-5.716651	1.556475
6	3.961922	-3.700940	0.838984
1	4.021250	-3.310939	1.518117
6	0.030869	-0.344545	3.8333996
1	-0.019210	1.335292	3.728260
1	0.849698	-0.044622	4.423451
1	-0.922647	-0.031995	4.403896
6	-0.030766	-2.463706	2.282256
1	-0.929417	-2.813872	2.803334
1	0.844628	-2.824238	2.834882
1	-0.415113	-2.501357	1.234386
6	-3.585349	1.370638	0.669241
6	8.803539	0.769010	0.029054
6	-4.798474	-0.761061	-0.038084
6	-3.576876	-1.361330	-0.101289
6	-3.289833	-2.810582	-0.099769
6	-2.331755	-3.330361	-0.991824
1	-1.837674	-2.657716	-1.687692
6	-2.007268	-2.000000	-1.000000
1	1.303141	5.072537	-1.723011
6	2.655805	5.564042	-0.116215
1	-2.414952	-6.623575	-0.123931
6	-3.589669	-5.059922	0.793100
1	-4.074508	-5.726797	1.501479
6	-3.906135	-3.702109	0.799629
1	-4.021203	-3.310128	1.518117
6	-6.090620	-1.008721	0.040972
6	-5.998213	-1.410498	1.019935
1	-6.768244	-0.765129	1.862749
6	-8.188259	-2.138570	1.011593
1	-8.874490	-2.056394	1.850331
6	-8.499421	-2.966109	-0.070141
1	-9.429517	-3.527944	-0.078624
6	-7.608611	-3.064609	-1.141300
1	-7.086174	-3.354588	-1.699192
6	-5.412804	-2.245867	-1.127084
1	-5.720170	-2.428904	-1.059636
6	-6.100403	1.497826	0.058601
6	-7.026399	1.390514	-0.992356
1	-6.805557	0.746126	-1.838337
6	-8.222231	2.108555	-0.964317
1	-8.012151	2.004141	-1.799635
6	-8.521673	2.934660	0.121678
1	9.456216	3.488811	0.145580
6	-7.613345	3.042233	1.177173
1	-7.838310	3.679744	2.028199
6	-6.411873	2.333741	1.143102
1	-5.705351	2.423864	1.963177
6	-3.307382	2.821277	0.045531
1	-2.414952	3.525972	0.099626
6	-1.798053	2.025996	1.576935
6	-2.018207	4.717754	0.882103
1	-1.261927	5.107947	1.557768
6	-2.682753	5.577134	0.004646
1	-2.444728	6.637247	-0.010104
6	-3.650942	5.059690	-0.860201
1	-4.165861	5.716632	-1.556548
6	-3.961848	3.700927	-0.839030
1	-4.712417	3.310529	-1.518575

Table S6. Optimized geometry of compound **3** (single molecule) at B3LYP/6-31G (d).

Atom number	x	y	z
14	2.296301	-0.126054	0.148126
8	-1.389894	0.020381	1.219102
14	-0.148696	0.440314	-2.223642
8	1.306942	0.356655	-1.444717
14	2.296334	0.126102	-0.148377
8	1.389907	-0.020324	1.219140
14	0.148737	-0.440204	2.223421
8	-1.306855	-0.356505	1.444438
6	0.395695	-2.187451	1.844463
6	0.677677	-3.110119	2.379899
1	1.597614	-2.883347	2.379882
6	0.449942	-4.422242	3.339714
1	-1.261269	-5.144233	3.300299
6	0.777599	-4.774970	3.901383
1	0.932429	-5.720220	4.130372
6	1.817881	-3.842453	3.941407
1	2.776105	-4.112279	3.778765
6	1.626250	-2.552388	3.411388
1	2.434441	-4.852172	4.455284
6	0.133471	0.795848	3.631595
6	-1.031193	0.909000	1.399202
1	-1.958535	0.457914	4.111879
6	-1.042662	1.865626	5.063703
1	-1.954784	2.003263	6.051186
6	0.116804	2.564756	5.832851
1	0.109918	3.247148	6.678755
6	1.281554	2.393997	5.808901
1	2.189134	2.923981	5.335508
6	1.290590	1.506047	4.001315
1	2.206305	1.378491	3.429702
6	3.837372	1.398181	3.181389
6	4.770683	0.703565	-0.205776
6	4.815382	0.810684	-0.048056
6	3.613269	1.454429	-0.007480
6	3.389394	1.990386	0.002579
1	4.141973	3.816737	0.748984
1	4.971572	3.446303	-1.340936
6	3.848693	5.179453	-0.757014
6	4.460929	5.854822	-1.349262
6	2.730304	5.679777	-0.001967
1	2.457212	6.739745	-0.021706
6	1.986481	4.792651	0.724997
1	1.137601	5.161387	1.293723
6	2.232308	3.448388	0.723998
1	1.646338	2.752640	1.301122
6	6.133966	1.500303	0.060207
6	7.083778	1.434425	-0.972829
1	8.511414	0.883515	-1.393575
6	8.301569	2.106092	-0.865452
1	9.020132	2.051671	-1.677910
6	8.538669	2.843701	0.284580
1	9.531141	3.300308	0.370903
6	7.666785	2.908267	1.322684
1	7.890000	3.475931	2.222158
6	6.443899	2.246247	1.208921
1	5.718735	2.303247	0.031572
6	6.040302	4.849004	0.323279
6	6.922433	-1.484888	0.857727
1	6.681346	-0.902693	1.742146
6	8.005065	-2.235246	0.823010
1	8.626247	-2.235558	1.666229
6	8.426105	-2.981576	-0.309868
1	9.345099	-3.560822	-0.336933
6	7.565555	-2.976538	-1.409818
1	7.813300	-3.552307	-2.208904
6	6.383589	-2.235743	-1.372173
1	5.714374	-2.238745	-2.227631
6	3.225434	-2.714816	-0.446933
6	2.237377	-3.143816	-1.388626
1	1.809424	-2.415750	-2.050066
6	1.974998	-4.496950	-1.542357
1	1.263995	-4.805778	-2.304421
6	2.578226	-5.476007	-0.186646
1	2.378378	-6.501117	-0.822270
6	3.494902	-5.030304	0.252311
1	3.961264	-5.759464	0.910056
6	3.817779	-3.665685	0.383456
1	4.285369	-3.780707	1.166660
6	-0.395737	2.187602	-2.844539
6	0.683087	3.139963	-2.819031
1	1.598296	2.882760	-2.381997
6	0.482382	4.437111	-1.320865
1	1.261929	5.143690	-3.302344
6	-0.777702	4.775176	-3.903093
1	-0.924959	5.772250	-4.310215
6	-1.814041	3.847377	-3.943838
1	-2.776980	4.113363	-4.375592
6	-1.267353	2.564480	-3.416196
1	-2.449180	1.853118	-3.453095
6	-0.131559	-0.979700	-1.361444
1	1.031572	0.991284	0.398882
1	1.944440	-0.458951	-4.141060
6	1.043261	-1.866925	-5.468062
1	1.959390	-2.040557	-4.000030
6	0.166446	-2.566427	-5.833248
1	0.109745	-3.246752	-6.679206
6	1.284666	-2.381524	-5.089964
1	2.189437	-2.922441	-3.533585
1	2.189224	-1.505163	-0.003221
1	2.206553	-1.377119	-3.431054
6	3.576746	1.269450	0.331903
6	4.770690	0.703489	0.205958
1	4.835157	-0.001976	0.079490
6	-3.613180	-1.455419	0.007141
6	-3.365809	-2.910178	-0.003309
1	-4.141526	-3.316845	0.748383
6	4.479796	-3.348837	1.073733
1	3.848398	-5.179874	0.756030
6	-4.460424	-5.855038	1.348386
6	2.773529	-5.676989	0.013466
1	-2.547281	-6.379997	0.019470
6	1.989772	-4.792347	-0.726660
1	-1.138164	-5.161418	-1.295832
6	2.272529	-3.427667	-0.726267
1	1.667771	-2.752525	-1.305313
6	6.133807	-1.500303	-0.003511
6	-7.085607	-1.834773	0.972775
1	-8.640493	-0.860135	1.867809
6	8.301380	-2.107965	0.864359
1	-8.930179	-2.655350	1.679787
6	-8.598746	-2.843848	-0.284801
1	-9.550104	-3.361774	-0.370943
6	7.666745	-2.908161	-1.322995
1	7.830013	-3.347547	-2.223569
6	-6.443876	-2.246117	1.209196
1	5.718778	-2.302921	2.016069
6	6.044971	-1.479907	0.238947
1	6.932074	-1.849909	0.369211
6	-6.651668	0.903134	-1.741583
1	-8.099471	2.235231	-0.823747
6	8.762487	2.233985	-1.684873
1	8.435305	2.921526	-1.121348
6	-9.345350	3.560277	0.338853
6	-7.565896	2.975775	1.411254
1	7.812449	3.549932	1.300374
6	-6.835254	2.235106	1.373163
1	5.714207	2.237669	2.223119
6	-3.225504	2.710163	0.447358
1	-2.282967	3.143518	1.399090
6	1.808976	2.415273	2.049952
1	-1.974907	4.492222	1.529398
6	-1.263866	4.805237	2.304906
1	-2.578480	5.447520	0.717779
6	2.334065	6.501011	1.823779
1	-3.495345	5.038882	0.231019
6	3.961970	5.759835	-0.008366
1	-3.818174	6.368165	-0.382518
6	-4.530892	3.370826	-1.139495

## References

- [1] SMART; Bruker-AXS:Madison, WI, **2009**.
- [2] G.M. Sheldrick, *Acta Crystallogr. Sect.A: Found. Crystallogr.* **2008**, A64, 112-122.
- [3] J. C. de Mello, H. F. Wittmann, R. H. Friend, *Adv. Mater.* **1997**, 9, 230-232.
- [4] R. R. Hu, J. W. Y. Lam, J. Z. Liu, H. H. Y. Sung, I. D. Williams, Z. N. Yue, K. S. Wong, M. M. F. Yuen, B. Z. Tang, *Polym. Chem.* **2012**, 3, 1481-1489.
- [5] M. J. Frisch, G. W. Trucks, H. B. Schlegel, G. E. Scuseria, M. A. Robb, J. R. Cheeseman, G. Scalmani, V. Barone, B. Mennucci, G. A. Petersson, H. Nakatsuji, M. Caricato, X. Li, H. P. Hratchian, A. F. Izmaylov, J. Bloino, G. Zheng, J. L. Sonnenberg, M. Hada, M. Ehara, K. Toyota, R. Fukuda, J. Hasegawa, M. Ishida, T. Nakajima, Y. Honda, O. Kitao, H. Nakai, T. Vreven, J. A. Montgomery, Jr., J. E. Peralta, F. Ogliaro, M. Bearpark, J. J. Heyd, E. Brothers, K. N. Kudin, V. N. Staroverov, T. Keith, R. Kobayashi, J. Normand, K. Raghuvaran, A. Rendell, J. C. Burant, S. S. Iyengar, J. Tomasi, M. Cossi, N. Rega, J. M. Millam, M. Klene, J. E. Knox, J. B. Cross, V. Bakken, C. Adamo, J. Jaramillo, R. Gomperts, R. E. Stratmann, O. Yazyev, A. J. Austin, R. Cammi, C. Pomelli, J. W. Ochterski, R. L. Martin, K. Morokuma, V. G. Zakrzewski, G. A. Voth, P. Salvador, J. J. Dannenberg, S. Dapprich, A. D. Daniels, O. Farkas, J. B. Foresman, J. V. Ortiz, J. Cioslowski, and D. J. Fox. *EM64L-Gaussian 09, Revision D.01*. Gaussian, Inc., Wallingford CT, **2013**.
- [6] (a) R. G. Parr, W. Yang, *Density Functional Theory of Atoms and Molecules*, Oxford University Press, Oxford, **1989**. (b) M. E. Casida in *Recent Advances in Density Functional Methods, Part I* (Ed.: D. P. Chon), World Scientific, Singapore, **1995**, pp.155-192.
- [7] W.C. Joo, J.H. Hong, S. B. Choi, H.E. Son, *J. Organomet. Chem.*, **1990**, 391, 27-36.
- [8] I. Toulokhonova, R. P. Zhao, M. Kozee, R. West, *Main. Group. Met. Chem.*, **2001**, 24, 737-744
- [9] Y. J. Cai, K. Samedov, H. Albright, B. S. Dolinar, I. A. Guzei, H. Rongrong, C. Zhang and R. West, *Chem. Eur. J.*, **2014**. Submitted.
- [10] JobinYvon Horiba. "A Guide to Recording Fluorescence Quantum Yields".  
<http://www.horiba.com/uk/scientific/products/fluorescence-spectroscopy/application-notes/quantum-yields/>
- [11] S. Dhami, A. J. de Mello, G. Rumbles, S. M. Bishop, D. Phillips and A. Beeby. Phthalocyanine fluorescence at high concentration: dimers or reabsorption effect? *Photochem.Photobiol.*, **1995**, 61, 341.
- [12] J. W. Eastman. "Quantitative spectrofluorimetry-the fluorescence quantum yield of quinine sulfate". *Photochem.Photobiol.*, **1967**, 6, 55-72.
- [13] R. U. Kadam, D. Garg, J. Schwartz, R. Visini, M. Sattler, A. Stocker, T. Darbre, J. L. Reymond, *ACS. Chem. Biol.* **2013**, 8, 1925-1930.
- [14] S. J. Hamodrakas, P. N. Kanellopoulos, K. Pavlou, P. A. Tucker, *J. Struct. Biol.* **1997**, 118 (1), 23-30.
- [15] (a) C. Janiak, *J. Chem. Soc., Dalton. Trans.* **2000**, 3885-3896; (b) S. Alvarez, *J. Chem. Soc., Dalton. Trans.* **2013**, 42, 8617-8636.